

5-1-2012

Modeling Total Suspended Solids in Combined Sewer Systems

Weilan Zhang

Southern Illinois University Carbondale, weilanzhang@siu.edu

Follow this and additional works at: <http://opensiuc.lib.siu.edu/theses>

Recommended Citation

Zhang, Weilan, "Modeling Total Suspended Solids in Combined Sewer Systems" (2012). *Theses*. Paper 803.

This Open Access Thesis is brought to you for free and open access by the Theses and Dissertations at OpenSIUC. It has been accepted for inclusion in Theses by an authorized administrator of OpenSIUC. For more information, please contact opensiuc@lib.siu.edu.

MODELING TOTAL SUSPENDED SOLIDS IN COMBINED SEWER SYSTEMS

by

Weilan Zhang

B.S., Chongqing University, 2010

A Thesis

Submitted in Partial Fulfillment of the Requirements for the
Master of Science

Department of Civil and Environmental Engineering
in the Graduate School
Southern Illinois University Carbondale
May 2012

THESIS APPROVAL

MODELING TOTAL SUSPENDED SOLIDS IN COMBINED SEWER SYSTEMS

by

Weilan Zhang

A Thesis Submitted in Partial
Fulfillment of the Requirements
for the Degree of
Master of Science
in the field of Civil Engineering

Approved by:

Dr. Lizette Chevalier, Chair

Dr. Bruce DeVantier, Co-chair

Dr. Xingmao Ma

Graduate School
Southern Illinois University Carbondale
April 3, 2012

AN ABSTRACT OF THE THESIS OF

WEILAN ZHANG, for the Master of Science degree in CIVIL ENGINEERING,
presented on April 3, 2012, at Southern Illinois University Carbondale.

TITLE: MODELING TOTAL SUSPENDED SOLIDS IN COMBINED SEWER
SYSTEMS.

MAJOR PROFESSOR: Dr. Lizette R. Chevalier

The untreated overflow of combined sewer system contains a variety of pollutants that can contaminate the receiving water body. Total suspended solids (TSS) transported in the sewer networks can adsorb these pollutants and become the main contaminant source. Existing models contain a numerous formulas that make the calculation process complex and time consuming. A simplified model was presented in this thesis to simulate the process of TSS transport in combined sewer pipes.

The combined sewer system evaluated was a combination of an existing sewer system in Le Marais and an example system provided with the Storm Water Management Model (SWMM). SWMM was used in this research to simulate the rainfall event, pollutant build-up and wash-off process, and to provide hydraulic calculations for the combined sewer system. A spreadsheet model was created to calculate the TSS concentration profile and flow velocity profile. The total TSS transport rate was computed using a numerical estimation of the integral of the concentration in the cross-section area multiplied by the velocity.

The flow depth, velocity, and Froude number of each pipe was calculated to show that the combined sewer system was under proper working conditions. The first flush phenomenon was observed by plotting the TSS concentration pollutograph of the combined sewer system. From the TSS transport pollutograph, the maximum transport rate was found (0.2609 kg/s at 6:45). The study of TSS profile showed that the concentration distribution was based on the solid density. The TSS particle also affected the transport rate. A sensitivity analysis of particle size was conducted in this thesis. A second order polynomial was used to describe the relationship between median particle size d_{50} and TSS transport rate.

ACKNOWLEDGMENTS

Foremost, I would like to express my deepest gratitude to my advisor Dr. Lizette Chevalier and my co-advisor Dr. Bruce DeVantier. Their guidance and encouragement was fundamental for the completion of my graduate studies and research. This thesis would not have been possible without them. I would like to thank my thesis committee member, Dr. Xingmao Ma, for providing me with necessary support and mentoring me through my graduate studies. I am also very grateful for the CEE faculties, staffs and all my SIUC classmates for their help and encouragement in the two years.

I would like to thank my dear friends Mr. Yinghua Lu, Mr. Hao-chun Pei, and Mr. Dennis Wang. My life in SIUC became more colorful and joyful with them.

I am very grateful for my supportive girlfriend, Ruiyan. Although there are 11,000 miles between us, her love and support are always there for me.

Lastly, I thank my parents whose love and persistent confidence in me. None of this would have been possible without their continued support and love.

TABLE OF CONTENTS

<u>CHAPTER</u>	<u>PAGE</u>
ABSTRACT	i
ACKNOWLEDGMENTS	iii
LIST OF TABLES.....	v
LIST OF FIGURES	vi
CHAPTERS	
CHAPTER 1 – Introduction	1
CHAPTER 2 – Background.....	4
CHAPTER 3 –Case study	20
CHAPTER 4 – Model development	27
CHAPTER 5 – Results	30
CHAPTER 6 – Conclusion	50
REFERENCES	52
VITA	57

LIST OF TABLES

<u>TABLE</u>	<u>PAGE</u>
Table 2.1: Physical properties of solids in different locations	5
Table 2.2: Settling velocity formulas for different particle size range.....	7
Table 2.3: Criteria of solids transport type	12
Table 3.1: Physical data of each pipe in example provided by SWMM	24
Table 5.1: Hydraulic calculation results of P10 during M17	36
Table 5.2: Hydraulic and TSS transport calculation results of all pipes at 6:45	48

LIST OF FIGURES

<u>TABLE</u>	<u>PAGE</u>
Figure 3.1: Illustration of combined sewer system in Le Marais	21
Figure 3.2: Hyetograph of event M17 in Le Marais.....	22
Figure 3.3: Schematic of example catchments and sewer system.....	23
Figure 3.4: Digitized hyetograph of event M17	25
Figure 3.5: Dry weather discharge of each subcatchment	25
Figure 4.1: Presentation of overall simplified model	29
Figure 5.1: Discharge and TSS concentration during M17	31
Figure 5.2: Measured discharge and TSS concentration in Le Marais during M17	31
Figure 5.3: Runoff curve of SC8 during M17	33
Figure 5.4: TSS concentration curve of SC8 during M17	33
Figure 5.5: Losses curve of SC8 during M17	34
Figure 5.6: The Froude numbers in P10 during M17	38
Figure 5.7: SWMM simulation status report.....	40
Figure 5.8: TSS transport rates in P10 during M17	42
Figure 5.9: TSS transport rates in Le Marais During M17	43
Figure 5.10(a): TSS concentration profile in P10 at 6:45 (density: 2400 kg/m ³)	45
Figure 5.10(b): TSS concentration profile in P10 at 6:45 (density: 1500 kg/m ³)	45

Figure 5.10(c): TSS concentration profile in P10 at 6:45	
(density: 3000 kg/m ³)	46
Figure 5.11: Flow velocity profile in P10 at 6:45	47
Figure 5.12: Sensitivity analysis of particle size	49

CHAPTER 1

INTRODUCTION

In many cities, early collection systems combined storm and sanitary sewers. Over time, increases in both population and impervious surfaces have increased the flow in these systems. During major storm events, the untreated overflow of these systems directly enters a receiving body of water. Numerous approaches have been used to try to collect and treat the overflow, including holding tanks. A sewer system, whether combined or strictly sanitary, may collect wastewater from residential, commercial or industrial sources. As such, the sewage water contains heavy metals, polycyclic aromatic hydrocarbons (PAH), bacteria and virus (Schlutter, 1999). When these contaminants are transported with stormwater into sewer system and finally discharge to the receiving waters, the contaminants negatively impact local water ecosystems. There is an increasing interest in reducing the amount of pollutants in the collected stormwater from heavy rainfall events.

Modeling solids transport in sewer pipes provides a tool for characterizing, analyzing, and predicting the fate of pollutants in the sewage. Usually, three types of solid transport are distinguished: the bed load transport, suspended load transport, and the wash load transport. The bed load is defined as the particles that slide, roll and saltate on the bed of a river or pipe (Bertrand-Krajewski, 2006). The suspended load is formed by particles that remain in suspension in the flow without definitive deposition (Bertrand-Krajewski, 2006). The wash load

includes those very fine particles that are permanently transported in the flow, without any deposition. Although many hydrological and hydraulic models are well established recently, there is still a challenge to calibrate water quality models and to make models more detailed. In past decades, researchers have established a series of models and formulas to describe the complex process based on very limited field data. For example, the Storm Water Management Model (SWMM) developed by US EPA provides models for accumulation of particles on the catchment and wash-off by rainfall (Rossman, 2004). Another software, MOUSE TRAP, developed by Danish Hydraulic Institute also comprises many formulas for calculating wash load transport, bed load transport and suspended load transport (DHI, 1993). Numerous parameters are required to simulate sediment transport so that the hydrodynamics and subsequent sediment transport can be described at a very detailed level. But increasing computational time consumption would become a critical drawback. For instance, when using the Sediment Transport Simulation (STSim) model takes one thousand simulations to model a complete sewer system of a small area community. Combined with the five calibration events, it takes more than two weeks to perform even on a fast PC (Schlutter, 1999). Therefore, a simplified approach method would be valuable and practical.

The main aim of this work was to present a simplified model to predict the sediment transport rate in combined sewer pipe. Particle size distribution and particle density are very significant factors in transport models. It varies based on

the sewer location and pollutant source. A sensitivity analysis of the transport rate and concentration profiles in pipes has been conducted in this study.

CHAPTER 2

BACKGROUND

2.1 Solids sources and characteristics

Although this thesis is mainly focusing on numerical modeling of sewer sediment transport, a description of the sources and characteristics of solids in the environment and sewer system is presented.

Sediment in the environment can carry pollutants as well as being a pollutant itself. In sewers, this is more prevalent due to the characteristics of the waste stream. Ashley et al. (2004) classified pollutant sources of sewer system into 6 source groups: atmosphere, surfaces on the catchment, domestic sewage, industrial and commercial effluents, the environment of sewer pipes, and construction sites. Surface runoff, especially the street runoff, contributes the largest part of sediments into combined sewer or storm sewer system. A study in Karlsruhe, Germany (Xanthopoulos and Augustin 1992) showed that approximately 90% of the catchment sediments originated from street runoff. Small particles deposited from the atmosphere, soil erosion in catchment areas, leaves, and other roadside waste may also be a source of sediment on the catchment surface. Additional fine particles are deposited from atmosphere after a rain event. Ashley and Crabtree (1992) reported that, on average, approximately 90% of the sediments deposited on the surface have a grain size less than 80 μm , and 40% of the sediments are organic. Sediments from the catchment may also adsorb a number of substances, including heavy metals, organic micropollutants, PAH, nutrients, bacteria and viruses (Schlutter, 1999).

The particles size and organic content of the sediment depends on the location of the sewers, as a result of factors such as the traffic density, (Schlutter, 1999) and green coverage. Table 2.1 provides a brief summary of this variability.

Table 2.1 Physical properties of solids in different locations

Status	Median diameter d ₅₀ (µm)	Specific gravity
Deposited along road and curbs (Ashley et al. 1999)	300-400	2.6
Transported in Domestic sewage (Ashley et al. 1999)	30-40	1.5
Transported in Sewer during wet weather (Chebbo et al. 1989; Dastugue et al. 1990)	30-40	2.4
Deposited in sewers (Crabtree 1989; Ashley et al. 1999)	200-1000	2.6

In the Table 2.1, particles transported in sewers by rain are very fine (30 µm – 40 µm), so that they are transported essentially in suspension (Dastugue et al. 1990). Particles deposited in sewers are often transported in sewer pipes by rolling and saltating. The Envirogenics Company (1970) used a screening technique to study the physical and chemical properties of combined sewer overflow solids collected in San Francisco from April 1969 to May 1970. A total of 60 combined sewage composite samples were collected. A number of parameters that describe the characteristics of solids were analyzed through those samples. Their results show that 48.3% of the particles in the local combined sewer overflows were less than 74 µm in size. The percentage of the size range 74-295 µm was 21.8%. Only 13.9% of the particles were larger than 991 µm. Krantz and Russell (1973) also conducted particle size analysis and density measurements of solids in catch basins. Their research shows 31.9% of

the suspended materials were small than 44 μm . Moreover, the specific weights of particles had relatively wide range (0.8-2.6). If the size is higher than 2000 μm , all particle specific weights were in the range 1.05 to 1.25. When the size went down to 149-2000 μm , solids specific weight 1.25-2.6 had the greatest size distribution percentage and highest specific weight.

Settling velocity, defined as the final velocity when the drag force due to motion of the particle through the fluid is equal to the applied force, is also a main characteristic of sewer solids. It can be measured and is frequently represented by means of media settling velocity ω_{50} . Setting velocity can be also calculated from grain size and specific gravity based on following two assumptions (Bertrand-Krajewski, 2006): (1) the particle is spherical; (2) the particle is isolated in infinite water volume. Rubey proposed a formula in 1993 showed the relationship (equation 2.1) between settling velocity ω and other parameters:

$$w = F \sqrt{g \frac{\rho_s - \rho}{\rho} d} \quad (2.1)$$

where:

g [m/s²] : acceleration of gravity;

ρ [kg/m³] : density of water;

ρ_s [kg/m³] : density of the particle.

F [-] : the factor of Rubey given by Equation 2.2:

$$F = \left(\frac{2}{3} + \frac{36\nu^2}{\Delta g d^3} \right)^{1/2} - \left(\frac{36\nu^2}{\Delta g d^3} \right)^{1/2} \quad (2.2)$$

where ν is the kinematic viscosity of water, Δ is equal to $(\rho_s - \rho)/\rho$.

Usually, researchers adopt different equations for different particle size distributions. Table 2.2 shows the typical formulas people choose for each particle size range.

Table 2.2 Settling velocity formulas for different particle size range

Particle size range	Name	Formula	
$d < 100\text{-}150\ \mu\text{m}$	Stokes formula	$w = \frac{g\Delta d^2}{18\nu}$	(2.3)
$100\ \mu\text{m} < d < 1000\ \mu\text{m}$	Zanke formula (Zanke, 1977)	$w = 10 \frac{\nu}{d} \left[\left(1 + \frac{0.01g\Delta d^3}{\nu^2} \right)^{0.5} - 1 \right]$	(2.4)
$d > 1000\ \mu\text{m}$	van Rijn formula (van Rijn, 1984b)	$w = 1.1\sqrt{g\Delta d}$	(2.5)

2.2 Review of sediment transport process and existing modeling systems

In this study, several theories on sediment transport processes in sewer systems have been reviewed. Typically, there are three main steps that describe sediments transported from sources to outlet of combined sewer system: (1) the accumulation of sediments over study catchments; (2) the wash-off of these sediments by rainfall; (3) the transport, erosion and deposition in sewer pipes. For each step, researchers have already established models, which will be presented hereafter.

2.2.1 Model of sediments build-up in catchments

The estimate of accumulated mass is important and required for subsequently wash-off modeling. The sediments accumulating process on the

surface before the rain event can be simulated by build-up models. Many factors affect the build-up condition, such as the residual mass deposited on the surface after the last event, street cleaning practices, traffic intensity and traffic speed, vegetation, urbanization and surface characteristics. Two types empirical models are usually considered: linear function and exponential function (Schlutter, 1999). The following equations describe the linear build-up process, which is stopped at a maximum value m_{\max} (kg/ha).

$$m_a = \alpha_{\text{acc}} t \quad , \text{ when } m_a < m_{\max} \quad (2.6)$$

$$m_a = m_{\max} \quad , \text{ when } m_a \geq m_{\max}$$

where:

α_{acc} [kg/ha/day] :rate of accumulation;

t [day] :period after last rain event;

m_a [kg/ha] :mass deposited on the surface after time t .

For the exponential function, the build-up process is described by Equation 2.7.

$$m_a = \alpha_{\text{acc}} t^{\alpha_{\text{acc}_2}} \quad , \text{ when } m_a < m_{\max} \quad (2.7)$$

$$m_a = m_{\max} \quad , \text{ when } m_a \geq m_{\max}$$

where α_{acc_2} is a numerical coefficient.

In catchment and sewer systems a certain degree of sediment decay and removal will take place on the surface at the same time as the accumulation. As a result, there is a maximum limit for accumulated mass on the surface. To account for this, the parameter, α_{rem} (kg/ha/day) is used to depict the sediment removal rate. The removal rate α_{rem} depends on local wind velocity, traffic

intensity. In the SWMM, the following exponential build-up function was introduced (Gironas et al. 2009).

$$\frac{dm_a(t)}{dt} = \alpha_{acc} - \alpha_{rem} m_a(t) \quad (2.8)$$

Sometimes, in order to avoid differential calculations, the following exponential build-up equation is chosen in SWMM (Gironas et al. 2009).

$$m_a = m_{\max}(1 - e^{-\alpha_{rem}t}) \quad (2.9)$$

Moreover, an asymptotic model shown in Equation 2.10 is also suggested (Schlutter, 1999).

$$m_a = \frac{m_{\max}t}{\alpha_{acc} + t} \quad (2.10)$$

Calibrating these functions using local data before applying them is necessary. Typically, the time to reach the equilibrium between accumulation and removal of sediments is about 5 to 20 day (Ashley et al. 1999). Ellis (1986) reported that it took 5 days to achieve the equilibrium condition in London. Ashley et al. (1999) estimated the average accumulation rate is in the range of 95-3200 kg/ha/year.

2.2.2 Model of wash-off by rainfall

After a rainfall event, the rainwater washes off the accumulation on the surface and transports the sediment to the combined sewer system or storm system. Rainfall intensity, duration, sediment characteristics, surface conditions, area, and slope of the surface affect these processes. Soil erosion also can

contribute pollutants to a sewer system, but in regions where an area is highly developed urban, the effects caused by soil erosion can be ignored.

Three methods are applied in SWMM to present the wash-off process: event mean concentrations (EMCs), rating curves, and exponential wash-off equation (Gironas et al., 2009). EMC assumes that each pollutant has a constant runoff concentration throughout the simulation. Rating curves produce the wash-off as functions of the run-off rate only (Gironas et al., 2009). Both EMCs and rating curves do not require build-up functions to represent the pollutant concentrations. The third approach used in SWMM is exponential wash-off function, which is shown in Equation 2.11.

$$W = C_1 \cdot q_{wo}^{C_2} \cdot B \quad (2.11)$$

where:

- W [lbs/hr] : rate of pollutant load washed off at time t;
- C_1 [(in/hr)^{-C₂}(hr)⁻¹]: wash-off coefficient;
- C_2 [-] : wash-off exponent;
- q_{wo} [in/hr] : runoff rate per unit area at time t;
- B [lbs] : pollutant buildup remaining on the surface at time t.

In SWMM, the value of exponent C_2 is in the range between 1.1 and 2.6, with most values around 2 (Vanoni, 1975).

Servat proposed a model derived based on field data (cited by Bertrand-Krajewski, 2006):

$$m_e = \alpha_w m_a^{c1} I_{max}^{c2} V^{c3} \quad (2.12)$$

where

α_w	[mm ⁻¹]	: wash-off coefficient;
m_e	[kg]	: washed off mass;
m_a	[kg]	: accumulated mass at the initiation of the rain;
$I_{\max 5}$	[mm/h]	: maximum rainfall intensity during a time step of 5 min;
V	[m ³]	: runoff volume;
$c1, c2, c3$	[-]	: numerical coefficients.

If the direct dependency on rainfall intensity needs to be avoided, the NPS (Non Point Source) model proposed by Litwin and Donigian (1978) can be applied.

$$m_e(t) = \alpha_w Q_s^{c1}, \text{ when } m_e(t) < m_a(t) \quad (2.13)$$

$$m_e(t) = m_a(t), \text{ when } m_e(t) \geq m_a(t)$$

where

$m_e(t)$	[kg/ha]	: washed off mass at time t;
$m_a(t)$	[kg/ha]	: accumulated mass at time t;
Q_s	[mm]	: surface runoff on impervious area;
$c1$	[-]	: numerical coefficient.

Generally, in the mentioned models, the rainfall intensity and runoff rate are the most critical factors in wash-off process. The build-up model and wash-off model could be integrated as a part of a bigger model. When the total transport is predominant in the whole simulation, the choice of wash-off model becomes less important (Schlutter, 1999).

2.2.3 Model of sediment transport in sewer pipes

Many researchers have presented sediment transport models, especially for fluvial hydraulics and solid transport in closed pipes (e.g. van Rijn, 1984a, b, Zug et al, 1998). Typically, three types of solid transport are distinguished: the bed load transport, the suspended load and the wash load. The total load is the sum of the three above loads. Many researchers only distinguish bed load and suspended load, assuming that the wash load is not really a mode of solid transport (Bertrand-Krajewski, 2006). The wash load is usually calculated by the advection-dispersion equation that is used for soluble substances. Settling velocity was used as a criteria by Raudkivi (1998) to distinguish the bed load and suspended load. The relationship is shown in table 2.3, where u^* is the shear velocity (m/s) and ω is settling velocity (m/s).

Table 2.3 Criteria of solids transport type

$\omega/u^* < 0.6$	Suspended load
$0.6 < \omega/u^* < 2$	Saltation
$2 < \omega/u^* < 6$	Bed load

Bed load formed during wet weather periods should decrease the hydraulic capacity of the pipe due to the reducing flow area and increasing bed resistance of pipes. Bed load transport can be modeled by conventional non-cohesive sediment transport formulas, such as Meyer-Peter Muller formula and Einstein formula. Lin and Le Guennec (1996) simplified Meyer-Peter Muller formula. This simplified formula can be applied for various particle sizes and shown in Equation 2.14, where q_B (kg/s/m) is the bed load transport rate per unit

width, θ is the shields parameter without units, d_e (m) is the effective diameter of particles.

$$q_B = 8(\theta - 0.047)^{3/2} \times \rho_s (\Delta g d_e^3)^{1/2} \quad (2.14)$$

The suspended load is a function of the local flow conditions and the composition of the bed material (Mark, 1995). The transport rate is traditionally calculated as the integral over cross-section area of concentration multiplied by the velocity. The formula is shown in Equation 2.15 (Bertrand-Krajewski, 2006), where a (m) is the thickness of the bed layer, z (m) is the distance from the pipe bottom.

$$q_s = \int_{z=a}^{z=y} C(z) \cdot u(z) dz \quad (2.15)$$

where:

- q_s [kg/s/m] : suspended load transport rate per unit width;
- y [m] : water depth in pipe;
- a [m] : the thickness of the bed layer;
- z [m] : the distance from the pipe bottom;
- $C(z)$ [mg/l] : solids concentration at distance z from the pipe bottom;
- $u(z)$ [m/s] : current velocity at distance z from the pipe bottom.

The current velocity at distant z , $u(z)$, is computed by Equation 2.16, where u^* (m/s) is the effective bed shear velocity and k_s (m) is the equivalent roughness (Bertrand-Krajewski, 2006).

$$u(z) = 2.5u^* \ln \left(\frac{30z}{k_s} \right) \quad (2.16)$$

For the vertical concentration profile $C(z)$, Rouse (1937) proposed a formula (Equation 2.17) to calculate it, where κ is the von Karman constant.

$$C(z) = C(a) \left(\frac{y-z}{z} \cdot \frac{a}{y-a} \right)^{\frac{w}{\kappa u_*}} \quad (2.17)$$

Leo C. van Rijn (1984a, b) established a series of models to compute the bed load, suspended load, and total load transport rate. The research showed that the bed load transport was the product of the saltation height, the particle velocity and the bed-load concentration. Intermediate relationships between transport rate and flow conditions were developed numerically from empirical laboratory data. Experiments with gravel particles that can be transported as bed load were used to calibrate the mathematical model. The verification analysis showed that about 77% of the predicted bed load transport rates from calculation were within 0.5 and 2.0 times the observed values. According to van Rijn's theory, the resulting procedure involved 6 steps to calculate the bed load transport rate. The first step is to calculate the dimensionless particle diameter D^* (Equation 2.18), where d_{50} (m) is the median diameter of particles.

$$D^* = d_{50} \left(\frac{\Delta g}{\nu^2} \right)^{1/3} \quad (2.18)$$

From there, the critical bed-shear velocity u_{*cr} (m/s) is calculated using the critical Shields parameter, where the critical Shields parameter is represented by a set of 5 relationships:

$$\begin{aligned}
D^* \leq 4 & \quad \theta_{cr} = 0.24 \cdot (D^*)^{-1} \\
4 < D^* \leq 10 & \quad \theta_{cr} = 0.14 \cdot (D^*)^{-0.64} \\
10 < D^* \leq 20 & \quad \theta_{cr} = 0.04 \cdot (D^*)^{-0.10} \\
20 < D^* \leq 150 & \quad \theta_{cr} = 0.013 \cdot (D^*)^{-0.29} \\
D^* > 150 & \quad \theta_{cr} = 0.055
\end{aligned} \tag{2.19}$$

$$u_{cr}^* = \sqrt{\theta_{cr} d_{50} \Delta g} \tag{2.20}$$

The next 3 steps calculate the Chezy coefficient related to grains C' , the effective bed-shear velocity $u^{* '}$ (with a maximum value equal to u^*), and the transport stage parameter T . Finally, the bed load transport rate, q_b is computed:

$$C' = 18 \log \left(\frac{12 R_h}{3 d_{90}} \right) \tag{2.21}$$

where R_h (m) is the hydraulic radius of the flow, d_{90} (m) is the diameter at which 90% of the particle is finer than.

$$u^{* '} = \frac{g^{1/2} U}{C'} \tag{2.22}$$

where U (m/s) is the mean flow velocity.

$$T = \frac{(u^{* '})^2 - (u_{cr}^*)^2}{(u_{cr}^*)^2} \tag{2.23}$$

$$q_B = 0.053 \frac{T^{2.1}}{D^{*0.3}} \rho_s (\Delta g)^{1/2} d_{50}^{3/2} \tag{2.24}$$

For suspended load transport, van Rijn (1984b) presented the same method as Equation 2.15. The author specified the reference concentration as a function of near-bed flow parameters and sediment properties. The research also investigated the parameters controlling the suspended load transport. The model developed by van Rijn can yield good results for predicting the sediment

transport of fine particles in the range 100 μm - 500 μm (van Rijn, 1984b). As shown in this paper, the method that computed the suspended load transport was based on the computation of the reference concentration from the bed load transport. The reference concentration is the solids concentration in the reference level. It was assumed that the reference level was equal to the equivalent roughness height of Nikuradse, because the bed form heights were not available for all experiments. The representative particle size of suspended sediment is also a significant parameter in the van Rijn model. Taking the computer costs into account, the Einstein-approach was used to determine a representative particle diameter of the suspended load. Moreover, this method also need to calculate following parameters: β -factor, ϕ -factor, F-factor, and suspension parameter Z and Z'. At last, the suspended load transport rate q_s can be obtain by Equation 2.25.

$$q_s = F \cdot U \cdot y \cdot C(a) \quad (2.25)$$

800 data points were used to verify this model and 76% of the predicted values were within 0.5 and 2 times the measured values.

Zug et al. (1998) applied the Velikanov model, a conceptual total load model, through a description of the solids behavior to study the sediment transport in combined sewer network. The objective of application was to reproduce the hydrographs and TSS concentration generated by any rainfall event. The Velikanov model was chosen by Zug et al. (1998) for its robustness, simple conceptual type of mathematical formula, reduced number of parameters and the possibility of differentiating three working rages that make it very suitable

for calibration and validation. M. Zug et al. (1998) integrated the Velikanov into a global model for solid production and transport in combined sewer system. The global model can be divided into four modules: hydrologic, hydraulic (Muskingum model), pollution (build-up, wash off and total load) and calibration function. The solids behavior was characterized by their settling velocity (w_s) and density (ρ_s) which varies between fine particles ($w_s=5.4$ m/h and $\rho_s=2000$ kg/m³) and coarse particles ($w_s=45$ m/h and $\rho_s=2650$ kg/m³). As known, the concentration of the transportable solids is not unique. The Velikanov model assumes the solids concentration varies in a range limited by two curves respectively corresponding to the maximum and minimum concentration able to be transported. This range can be calculated by the following equations:

$$\begin{aligned} C_{\min} &= \eta_{\min} \rho_s \rho_m (\rho_s - \rho)^{-1} \frac{U}{w} J \\ C_{\max} &= \eta_{\max} \rho_s \rho_m (\rho_s - \rho)^{-1} \frac{U}{w} J \end{aligned} \quad (2.26)$$

where η_{\min} and η_{\max} are the efficiency coefficient, ρ_m (kg/m³) is the density of the mixture liquid, J (m/m) is the slope of the energy grade line.

According to the two equations, three working conditions can be specified. If solids concentration $C < C_{\min}$, there is erosion in pipe until $C=C_{\min}$. If $C_{\min} < C < C_{\max}$, sediment would transport at concentration C without deposition or erosion. If $C > C_{\max}$, deposition would occur in pipe until $C= C_{\max}$. The Powell method is used to numerically optimize the calibration of Velikanov parameters. The model was applied to three sites in France, with reasonable results found for fitting of the real TSS pollutographs.

These above models are widely used for studying the complicated transport phenomena. Each model has been calibrated with its own data sets, while the data are respectively limited. So the comparison of the models is not straightforward (Bertrand-Krajewski, 2006). Collection of sufficiently precise field data is a challenge for future work.

2.3 The background of storm water management model (SWMM)

The SWMM model was first developed in 1971 by USEPA. The latest version is SWMM 5.0.022 and is available in public domain (USEPA, 2012). This free software is widely applied in urban areas throughout the world for planning, analysis and design runoff, combined sewers, sanitary sewers, and other drainage systems (Rossman, 2004). Three portions can be well simulated in this software: hydrological process, flow routing and water quality. For hydrological process, infiltration is modeled through the Horton, Green-Ampt or SCS curve Number method. Surface runoff is given by the Manning's equation (Gironas et al. 2009). For flow routing in pipes and channels, a user can choose the the equations SWMM uses: the steady flow routing; the kinematic wave routing; or the full dynamic wave routing. In the water quality portion, the pollutant can be modeled using build-up and wash-off equations presented in the previous section.

To initiate SWMM, the user must specify a default set of options and object properties, such as the software running environment. The user must then develop a network representation of the system under study. The user can edit

the properties of each object in the network. Analysis options, including data options, time step options, dynamic wave routing options, and interface file options, also need to be selected by the user. After running the simulation, the user can view results graphically or tabularly.

SWMM accounts for various hydrologic processes that produce runoff from urban areas (USEPA, 2012). SWMM contains a series of hydraulic models used to simulate the routing process of runoff and wastewater through the drainage system network of pipes, channels, storage/treatment units and diversion structures. In addition to modeling the generation and transport of runoff flows, SWMM can also estimate the production of pollutant loads associated with this runoff (USEPA, 2012).

In this work, the capabilities of SWMM to simulate time-varying rainfall processes, routing of wastewater and storm water in drainage network of pipes, pollutant buildup over different land uses, pollutant wash-off from specific land uses during storm event, and the routing of water quality constituents through the drainage system were utilized.

CHAPTER 3

CASE STUDY

The case study presented is a hypothetical system that merged two combined sewer systems: a real one and an example provided by SWMM.

The real combined sewer system is located in the Le Marais catchment, a business and shopping community in Paris. Le Marais is an old quarter with predominantly narrow one-way street, developed since the 17th century. The total area is approximately 42 ha. The shape of this catchment is more or less a rectangle, as shown by the boundary line (blue) in Figure 3.1. The east to west distance is approximately 800 m; the north to south distance is approximately 600 m. The (red) points indicate manholes and the connecting (green) lines indicate the combined sewer pipes. The average slope of the streets is 0.8%. The combined sewer in Le Marais is only a small fraction of whole system in Paris. The total length of the main sewers is 5.8 km. The slope of the main sewers is less than 1.5% (Schlutter 1999).

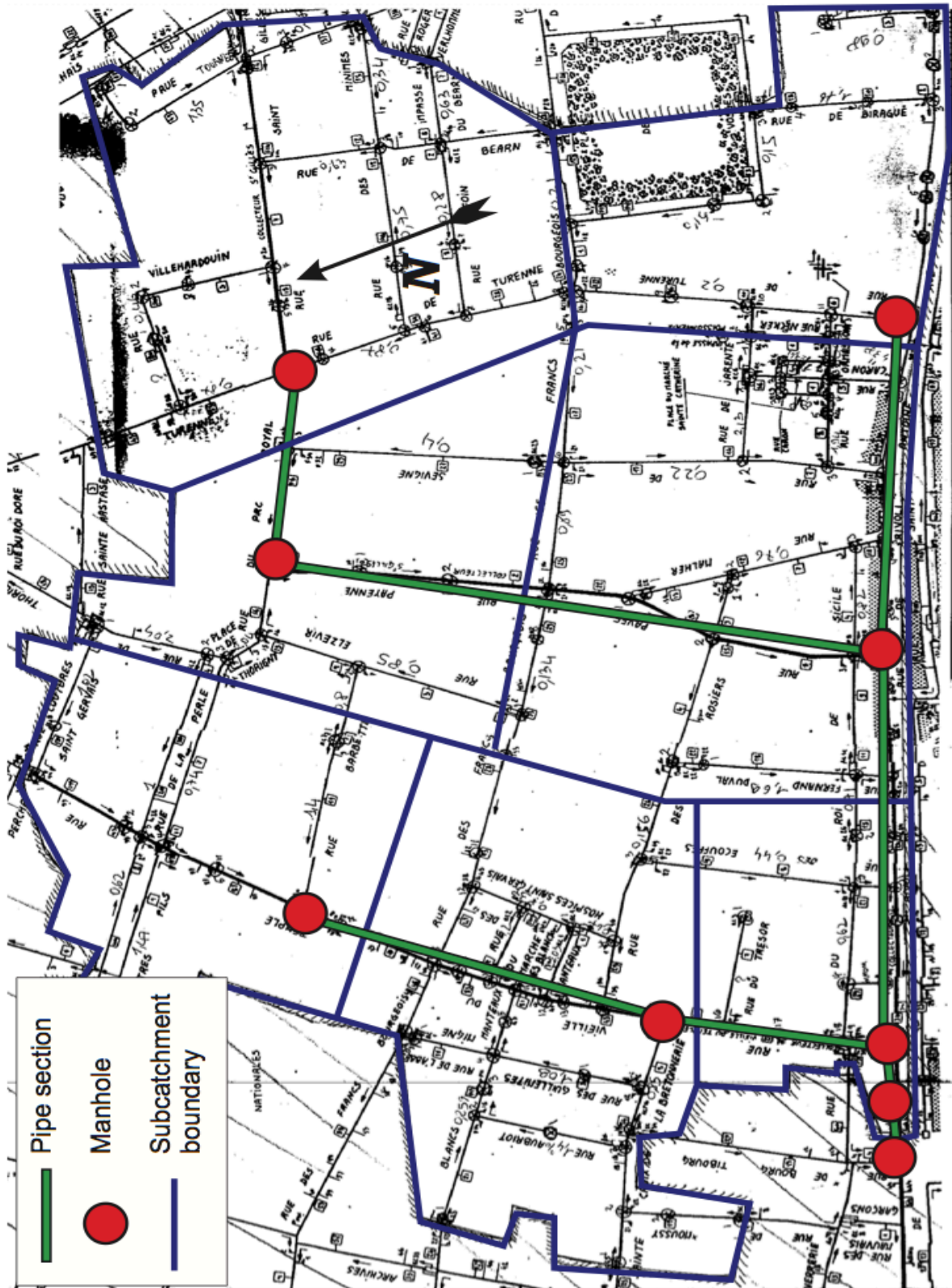


Figure 3.1 Illustration of combined sewer system in Le Marais

Schlutter (1999) reported the local rain intensity using a hyetograph (Figure 3.2). Thesis data were used for this study. The rainfall event that occurred on July 5, 1996 is referenced as M17. The duration of this rainfall was 321 minutes. The maximum intensity was 5.72 $\mu\text{m/s}$. Schlutter (1999) used this hyetograph to study the numerical modeling of sediment transport in the combined sewer system.

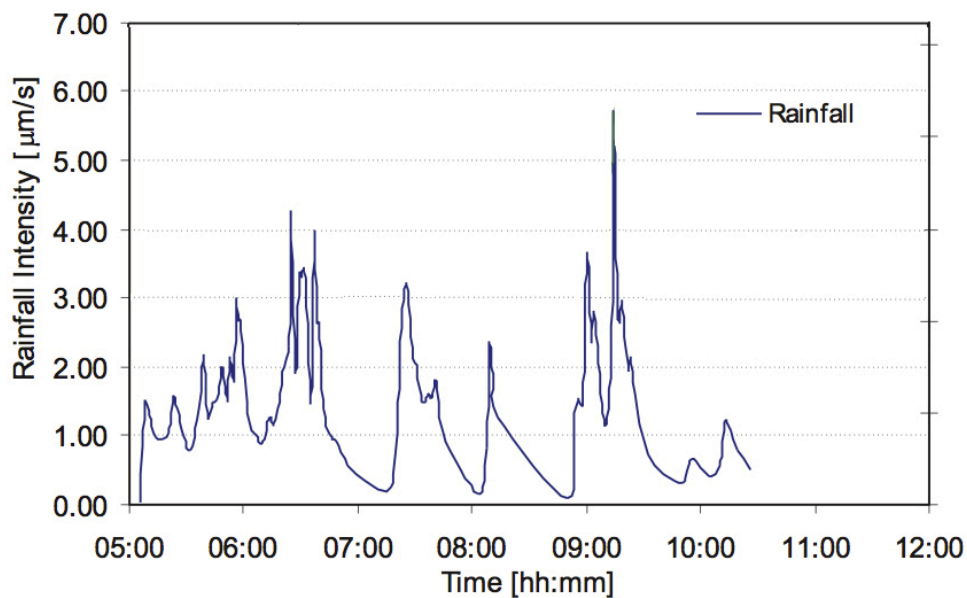


Figure 3.2 Hyetograph of event M17 in Le Marais

Figure 3.3 presents the SWMM example schematic, illustrating catchments, manholes, sewer pipes and outfall (Rossman, 2004). In this diagram, subcatchments are labeled as SC, manholes are labeled as MH, pipes are labeled as P and rain gages are labeled RG. The area of the catchment is approximately 40 ha, which is slightly smaller than the 42 ha of the Paris catchment. The Manning's n of all circular sewer pipes is 0.01. Detailed data

such as the elevation of manholes and outfall, the diameter and length of sewer pipes are summarized in Table 3.1.

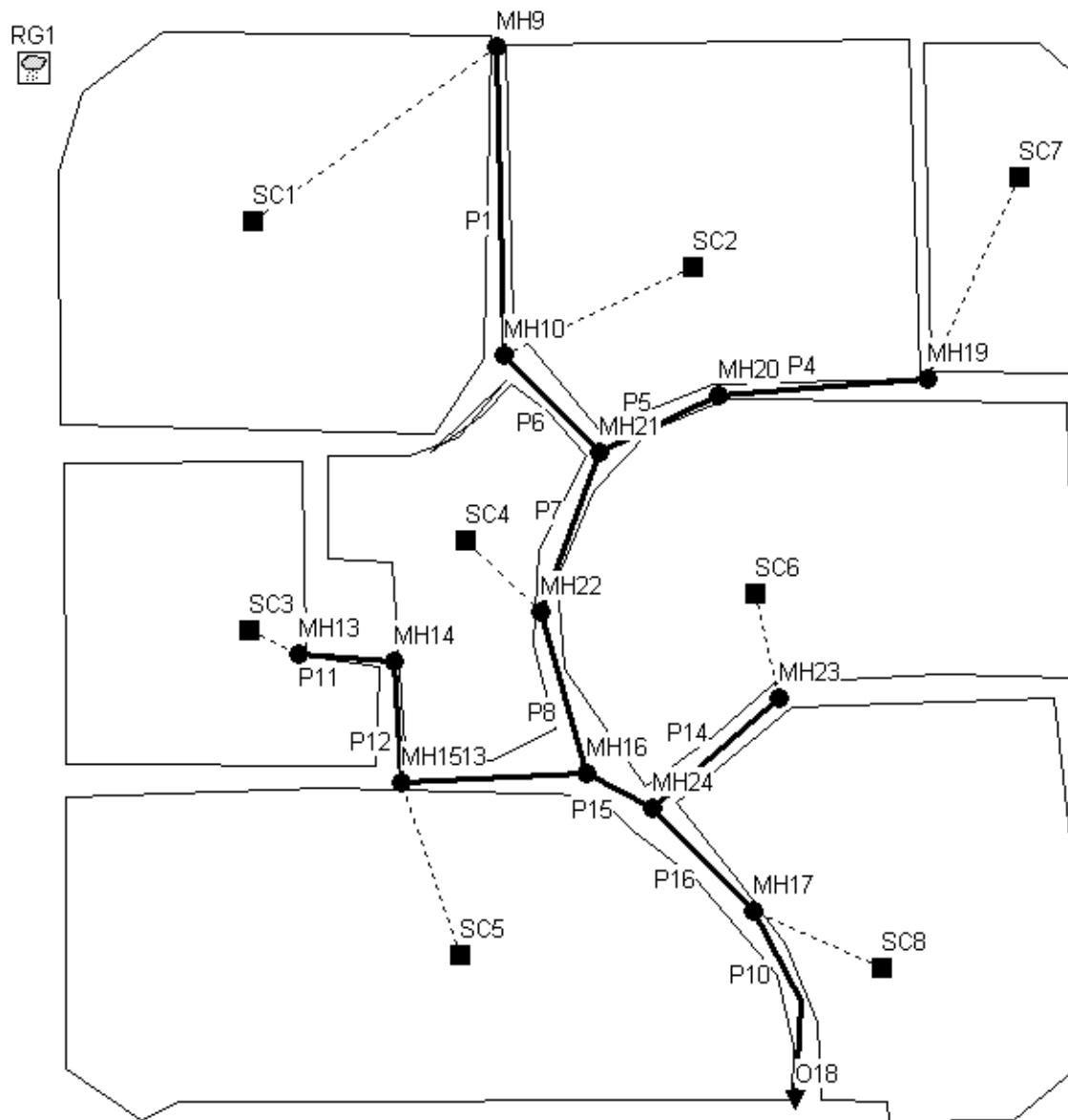


Figure 3.3 Schematic of example catchments and sewer system

Table 3.1 Physical data of each pipe in example provided by SWMM

Name	Max. Depth (m)	Length (m)	Slope (m/m)
P1	0.5	120	0.0417
P4	0.32	90	0.0556
P5	0.32	60	0.2500
P6	0.32	120	0.0417
P7	0.65	90	0.0333
P8	0.65	90	0.0222
P10	0.65	120	0.0417
P11	0.5	120	0.0417
P12	0.5	120	0.0250
P13	0.5	120	0.0167
P14	0.32	120	0.0500
P15	0.65	30	0.0333
P16	0.65	120	0.0333

The case study merged the data sets of the two systems. The catchments data and combined sewer system data were adopted from the example provided by SWMM, while the rainfall event data were from Figure 3.2. The rainfall event data in Le Marais can be digitized into SWMM in a time series format using 15 minutes intervals. The rainfall intensity was converted to mm/hr (Figure 3.4). The dry weather discharge of each subcatchment was also digitized from Le Marais data set into SWMM, which is shown in Figure 3.5.

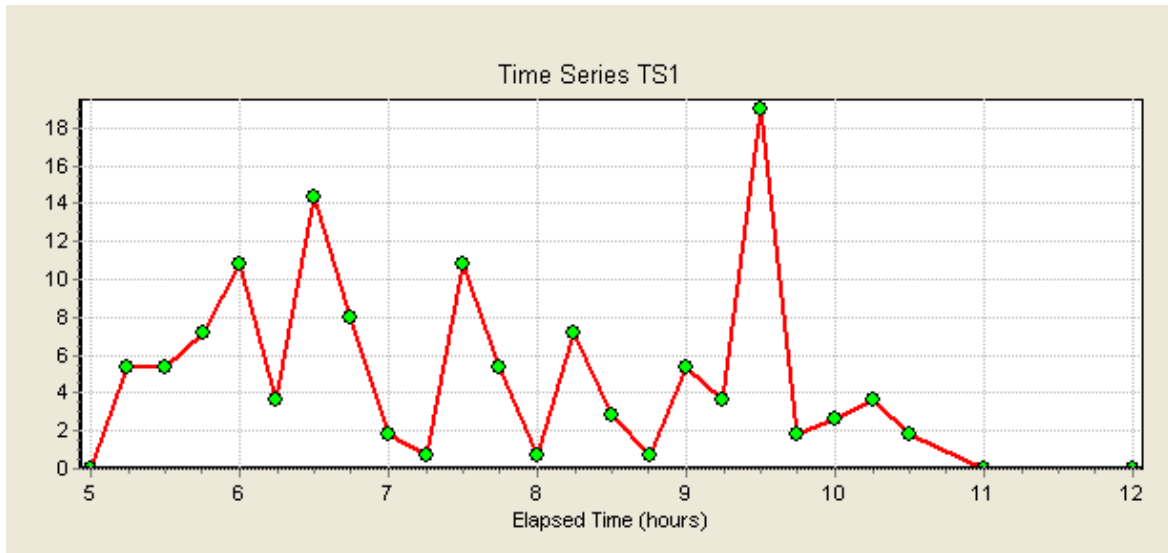


Figure 3.4 Digitized hyetograph of event M17

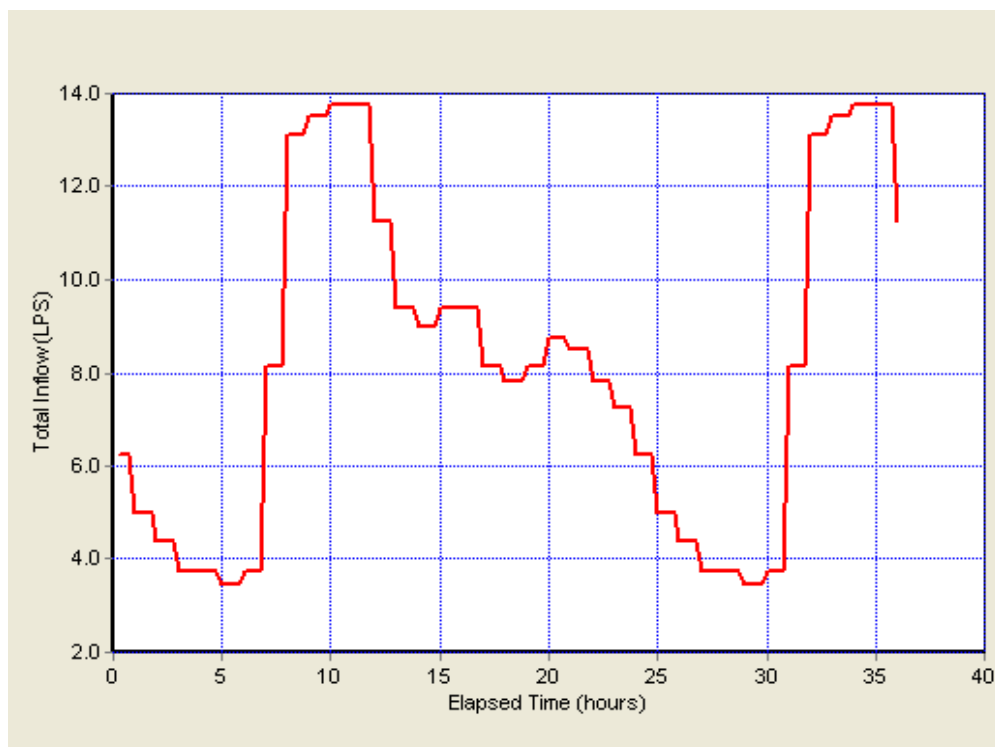


Figure 3.5 Dry weather discharge of each subcatchment

The catchment for the case study had a uniform slope of 1%, the percentage of impervious area was set at 80%, and manning's n for the impervious area was set at 0.003, and 0.1 in the pervious area. The infiltration of

the catchments was modeled by Horton method. All the catchment land uses were defined as residential. TSS was the only pollutant considered for this study. A power function was chosen to calculate the build-up of mass with a maximum value of 50 kg/ha. The power constant was set at 2. The wash-off process was described by exponential function. The wash-off coefficient was set at 0.1. The routing method used was the kinematic wave method.

CHAPTER 4

MODEL DEVELOPMENT

The flow chart shown in Figure 4.6 illustrates the process for evaluating the combined hypothetical catchment. Since the particle size of the suspended load was under 100 μm , the Rouse model and traditional integral equation (Equation 2.15) were adopted (Dalrymple et al., 1975). According to the Table 2.1 in previous chapter, the mean particle size d_{50} was assumed to be 40 μm and the specific gravity of the particle was set at 2.4.

The SWMM simulation outputs the hydraulic and water quality. The TSS concentration profile in pipes was computed by Rouse formula (Equation 2.17). In this equation, a is the thickness of the bed layer which can be approximated by $2d_{50}$ (DHI, 1983), z is the distance from the pipe bottom, ω is the settling velocity that can be calculated from table 2.2, κ is the von Karman constant and equal to 0.4 in this model, u^* is the bed shear velocity that can be calculated by equation 4.1 (Bertrand-Krajewski, 2006).

$$u^* = (gR_h I_r)^{0.5} \quad (4.1)$$

where R_h is the hydraulic radius and I_r is the slope of pipe.

$C(a)$ is the TSS concentration at a distance of a , which is the thickness of bed layer, from the bottom of the pipes. $C(a)$ was treated as the concentration at the bed of pipe in Rouse model. It was calculated in an EXCEL spreadsheet. Based on an initial value of a , a corresponding concentration profile was predicted. Based on the concentration profile, the mean concentration was

computed. An iterative process was applied where a value of $C(a)$ was used, and a new mean concentration was computed. The process was repeated until the mean concentration was equal to the value computed by SWMM. The value of $C(a)$ at the last iteration in EXCEL spreadsheet was the TSS concentration at the bed of pipe.

The logarithmic velocity profile in pipes, $u(z)$, was computed by equation 2.16. As mentioned in the previous chapter, k_s is the equivalent roughness and assumed to be equal to $2.5d_{50}$ (DHI, 1993). The u^* is the effective bed shear velocity and calculated by Equation 4.2.

$$u^* = \frac{g^{1/2} U}{C'} \quad (4.2)$$

where C' is the Chezy coefficient related to grains and calculated by Equation 4.3.

$$C' = 5.75 \sqrt{g} \log \left(\frac{12 R_h}{k_s} \right) \quad (4.3)$$

Finally, the TSS transport rate was computed by the integral equation 2.15. The integral calculation was determined by using the trapezoidal rule in EXCEL with a uniform grid of 0.0005 m.

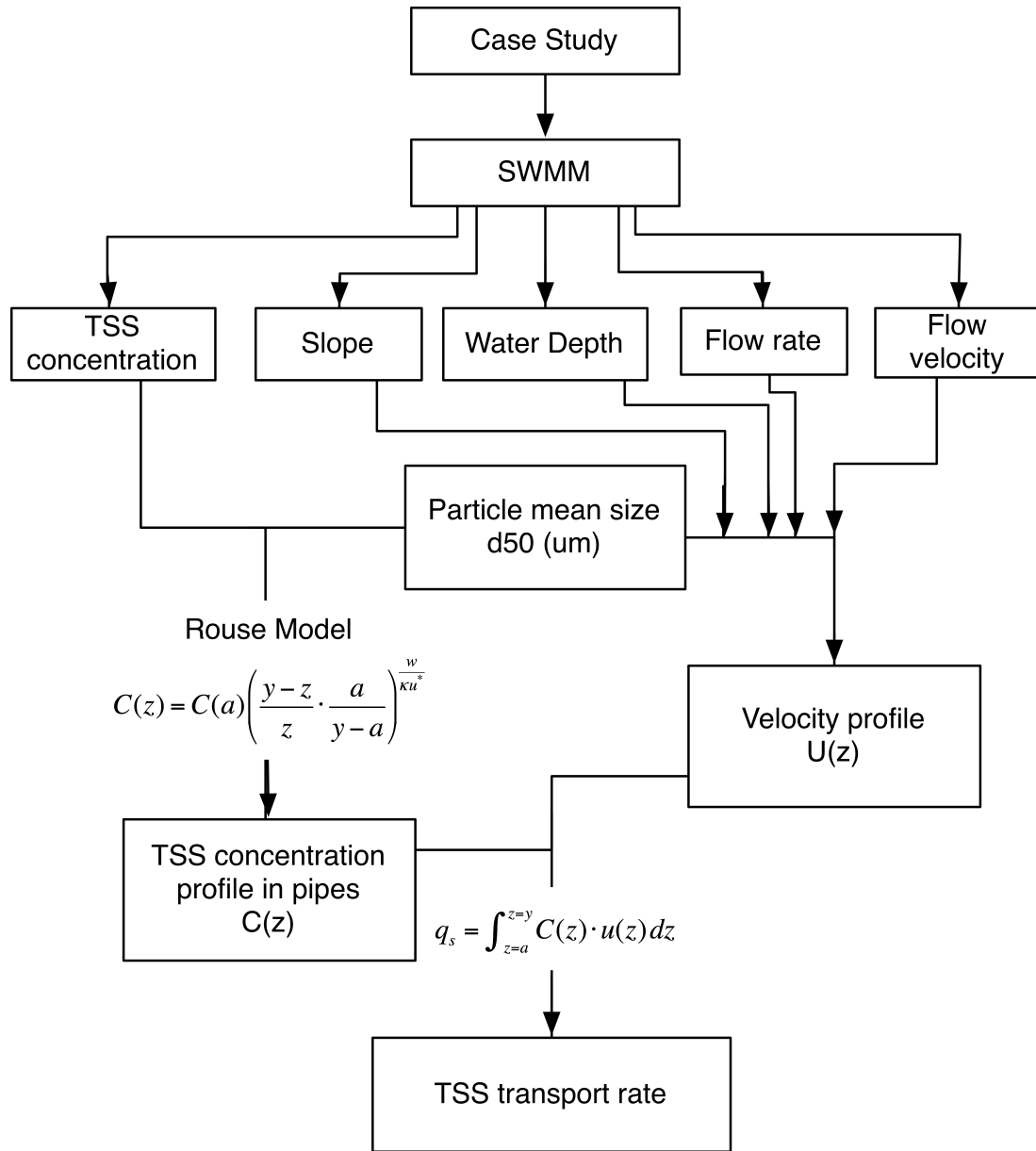


Figure 4.1 Presentation of overall simplified model

The TSS transport rates in the last pipe section of the whole combined sewer system (P10) were computed from 5:00 to 12:00. Then the TSS transport pollutograph was developed using a specified time interval (15 minutes). When the pollutograph reaches a peak, the TSS transport rates of other pipe sections also can be computed.

CHAPTER 5

RESULTS

In Figure 5.1, the discharge and TSS concentration curves for the last pipe section of case study system are presented. The data was calculated using SWMM. There are two peaks in the discharge curve. The maximum value of discharge was about $0.8 \text{ m}^3/\text{s}$ and occurs at nearly 10:00. The second peak of approximately $0.72 \text{ m}^3/\text{s}$ appeared earlier, between 6:45 to 7:00. For the TSS concentration curve, the peak concentration of approximately 425 mg/l occurred near 6:00. The original measured data in outfall of Le Marais combined sewer system are shown in Figure 5.2 (adopted from Schlutter, 1999). The shape of discharge and TSS concentration curves are very similar with results of the study (Figure 5.1.) The two peaks of discharge happened at 6:45 and 9:30, and both of them are approximately $0.75 \text{ m}^3/\text{s}$. The TSS concentration reached the maximum value of 424 mg/l at 5:45.

The comparison of the two curves demonstrated that the case study sewer system has very similar hydraulic and hydrology conditions with the existing combined sewer system in Le Marais. The conditions of two catchments, including the area and the land use, are also similar. So the combination of the two data sets (rainfall event data from Le Marais and combined sewer system data from SWMM example) was practical and can be used to in this study.

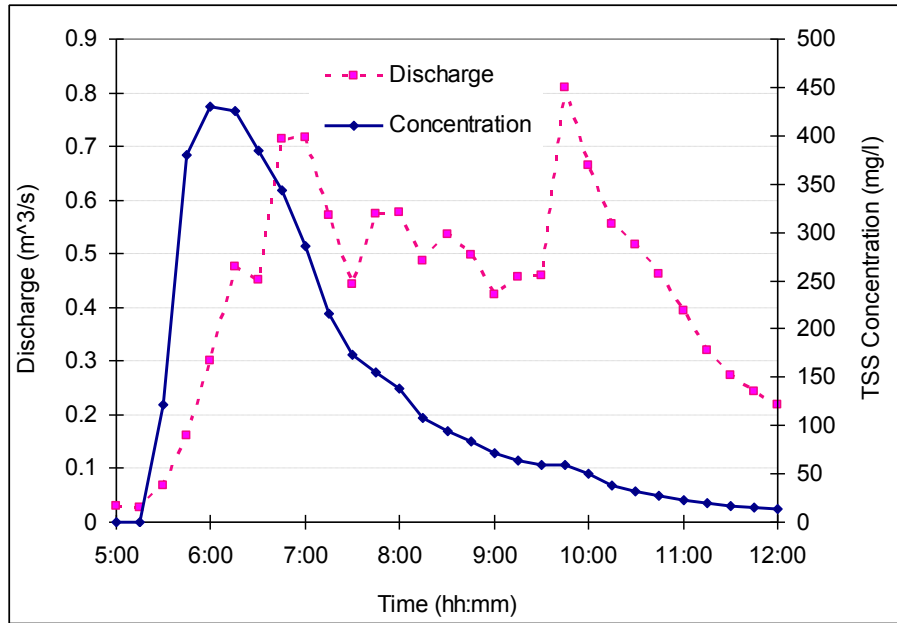


Figure 5.1 Discharge and TSS concentration during M17

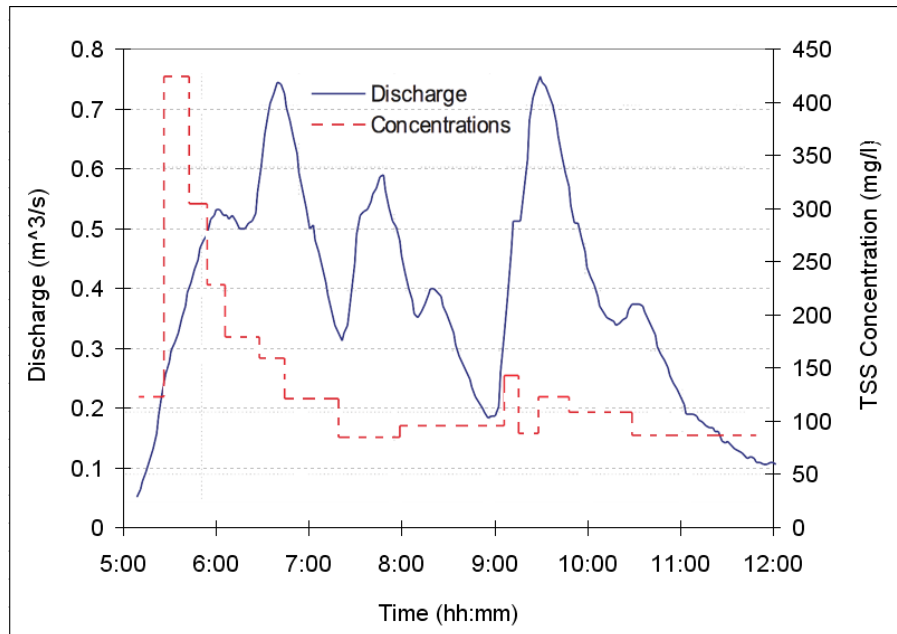


Figure 5.2 Measured discharge and TSS concentration in Le Marais during M17

The TSS source of the case study system was the all subcatchments in Figure 3.3. Figure 5.3 and figure 5.4 show the runoff curve and TSS concentration curve in subcatchment SC8. The runoff is in direct proportion to the area of corresponding subcatchment. The area of SC8 is 5 ha, so that the

highest value in this subcatchment was 110 l/s. The peak value of TSS concentration in SC8 runoff was 500 mg/l. It was higher than the TSS concentration in the corresponding receiving pipe, which was 450 mg/l. This dilution in the pipe was due to the wet weather inflow from the subcatchment. It is obvious that the TSS concentration during initial period of stormwater runoff was substantially higher than during later periods. This phenomenon is called the first flush (Gupta and Saul, 1996). During the first flush process, enormous quantity of pollutants, including TSS, are transported by stormwater runoff and discharged into the receiving waters or receiving sewer system. For this reason, TSS has been used as an indicator of pollution for urban drainage design by many researchers (Hogland et al., 1984, Lessard et al., 1982, Verbanck et al., 1994). Hogland et al. (1984) reported that heavy metals, COD and organic compounds would adsorb to the suspended solid. These suspended solids connected with diverse pollutants found in TSS in the combined sewer system. Therefore, the first flush may introduce the largest proportion of the pollution to the sewer system. Bertrand et al. (1998) concluded that the first flush results in a pollutants concentration peak at the beginning of rainfall event. The TSS concentration peak that happened nearly 6:00 in Figure 5.1 supports this conclusion.

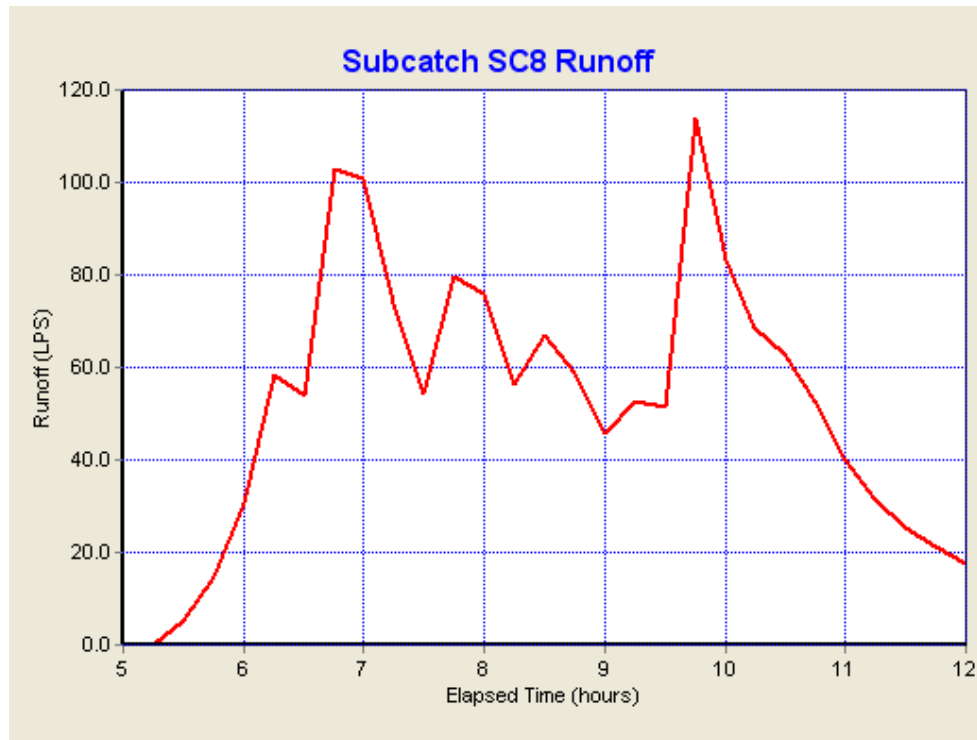


Figure 5.3 Runoff curve of SC8 during M17

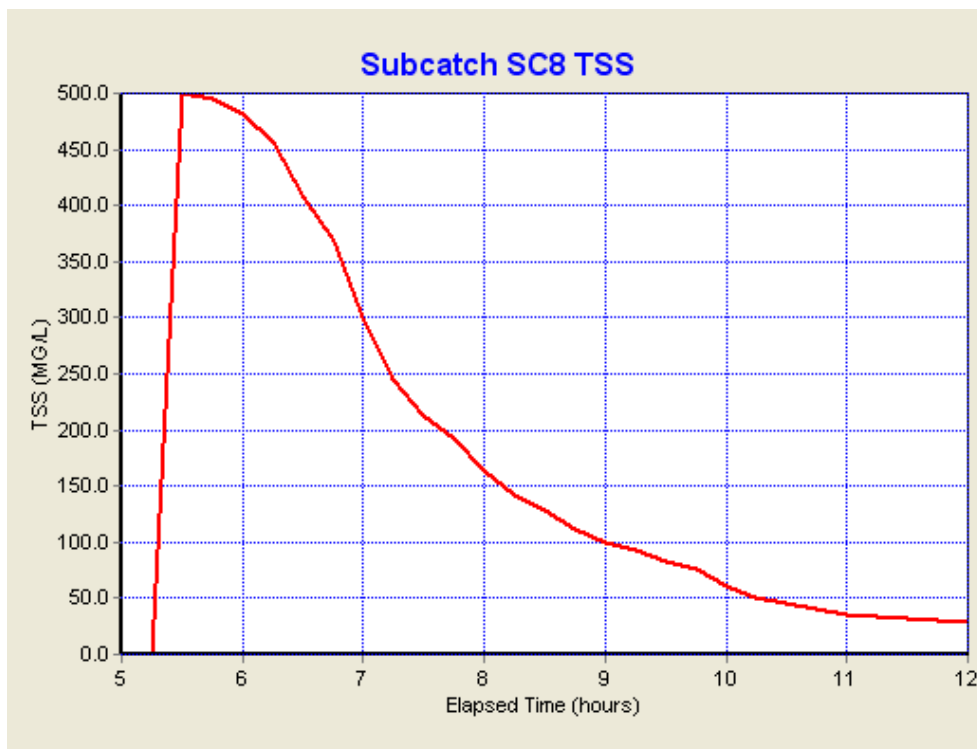


Figure 5.4 TSS concentration curve of SC8 during M17

Runoff losses caused by infiltration and evaporation can occur during a rainfall. Figure 5.5 shows the losses of SC8 during the simulation. The maximum loss was roughly 0.11 mm/hr. The loss became a constant 0.06 mm/hr after 6:00. According to the Figure 3.2, the average intensity during the rainfall period was roughly 5.4 mm/hr, and the maximum value was approximately 64.8 mm/hr. These losses were minor compared to the rainfall intensity.

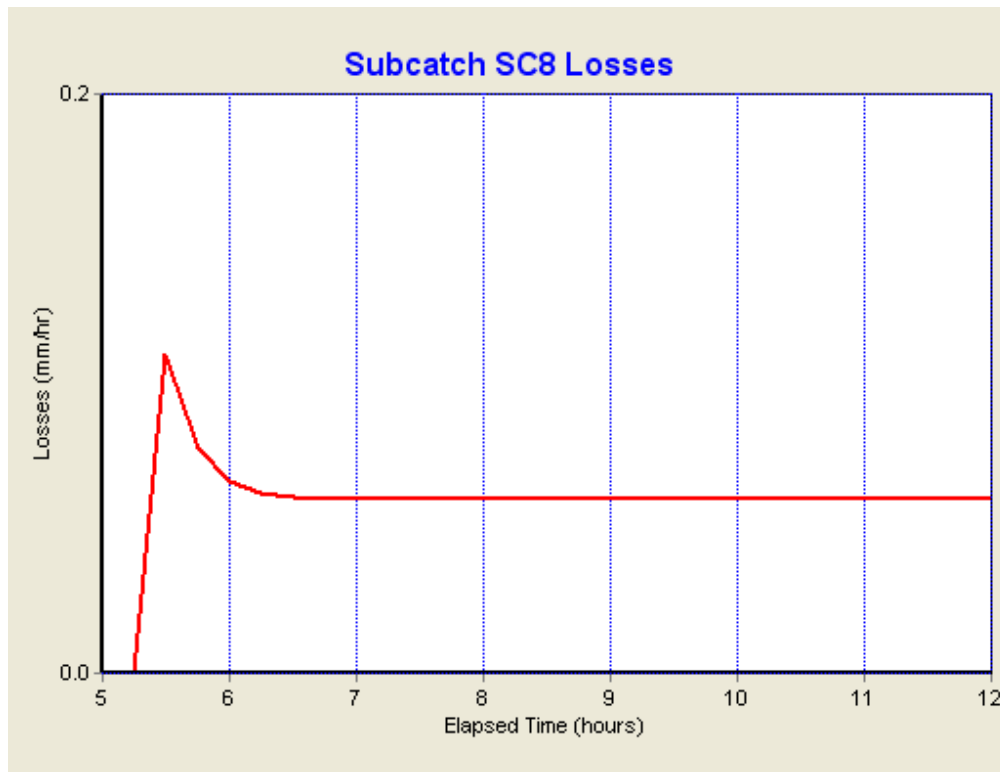


Figure 5.5 Losses curve of SC8 during M17

The hydraulic results of the SWMM simulation for the last pipe section (P10) are shown in table 5.1. The maximum flow depth of P10 during the simulation was 0.4136 m at 9:45, and the minimum flow depth was 0.0723 m after 5:15. SWMM uses an indicator called capacity to describe the ratio of flow depth and pipe diameter. The diameter of P10 was 0.65 m. So the capacity of pipe was in the range of 0.111 m/m to 0.636 m/m. The Denver Storm Drainage

Criteria Manual (City and County of Denver, 2006) reports that the maximum allowable velocity in all storm sewers shall be 18 ft/sec (5.49 m/s) and the minimum velocity shall be 3 ft/sec (0.91 m/s) at half-full or full-conduit flow conditions. The minimum flow velocity in P10 was 1.3637 m/s at 5:15, while the maximum flow velocity was 3.6394 m/s at 9:45. Table 5.1 summarizes the velocity between 5 -12 hours, indicating that the velocity meets requirements of the code.

Table 5.1 Hydraulic calculation results of P10 during M17

Time	Flow (l/s)	Depth (m)	Velocity (m/s)
5:00	29.9412	0.0731	1.4556
5:15	27.6045	0.0723	1.3637
5:30	67.6538	0.1099	1.8215
5:45	161.2107	0.1679	2.3716
6:00	301.257	0.2319	2.8348
6:15	476.8026	0.2982	3.2104
6:30	450.8162	0.2878	3.18
6:45	714.5751	0.3803	3.543
7:00	715.8672	0.3796	3.5573
7:15	571.7698	0.3293	3.3885
7:30	443.9251	0.2847	3.1755
7:45	574.3486	0.3319	3.3699
8:00	575.9276	0.3321	3.3772
8:15	488.1527	0.3004	3.2554
8:30	535.6407	0.318	3.319
8:45	498.3842	0.3044	3.2679
9:00	423.4985	0.2775	3.1324
9:15	456.5367	0.29	3.1881
9:30	458.9447	0.2907	3.1947
9:45	810.1982	0.4134	3.6394
10:00	665.6807	0.3612	3.5147
10:15	555.7772	0.3243	3.3595
10:30	515.9244	0.3108	3.2924
10:45	461.1378	0.2911	3.2039
11:00	394.1581	0.2665	3.075
11:15	319.7669	0.238	2.904
11:30	274.6862	0.2196	2.7842
11:45	242.8788	0.2058	2.6924
12:00	217.7803	0.1941	2.6179

The Froude number is a dimensionless parameter defined as the ratio of the inertia force on an element of fluid to the weight of the fluid element. In fluid mechanics, the Froude number is used to determine the resistance of a partially submerged object moving through water, and permits the comparison of objects

of different sizes (Crowe et al., 2009). Equation 5.1 shows how to calculate the Froude number in circular pipes, where T is top water surface width and A is the area of section flow.

$$F = \frac{U}{\sqrt{g \frac{A}{T}}} \quad (5.1)$$

The Froude number can be used to describe different flow regimes in open channel flow. If the Froude number is larger than 1, the flow is called supercritical flow. In this case, the flow velocity is larger than the wave velocity. If the Froude number is less than 1, the flow is called subcritical flow. When the Froude number is equal to 1, the flow is unstable and often transforms to supercritical or subcritical flow. The Froude number of the flow in P10 at each time step was calculated by SWMM during the simulation of rainfall M17. The Froude number curve is shown in figure 5.6. The Froude numbers is consistently larger than 1. The flow was only supercritical during whole rainfall process. According to Hager (1999), if the Froude number is larger than 3, the flow can be classified as hypercritical flow which is strong and unstable with potential damage. The supercritical flow would breakdown in sewer manholes due to the change of hydraulic conditions. Hager and Gissonni (2005) reported that the breakdown of supercritical flow in both storm and combined sewer manholes might be dangerous and cause shockwaves and hydraulic jumps. Shockwaves would increase the depth of medium flow section, even beyond the shock front. The hydraulic jump is a significant problem in sewers that would result in water hammer and backwater effect, which may geyser the wastewater out of manhole

onto public space (Hager and Gissoni, 2005). All the Froude numbers during rainfall event M17 were under 2.3. Compared to the hypercritical flow, the level of damage caused by shockwaves and backwater would be relatively low.

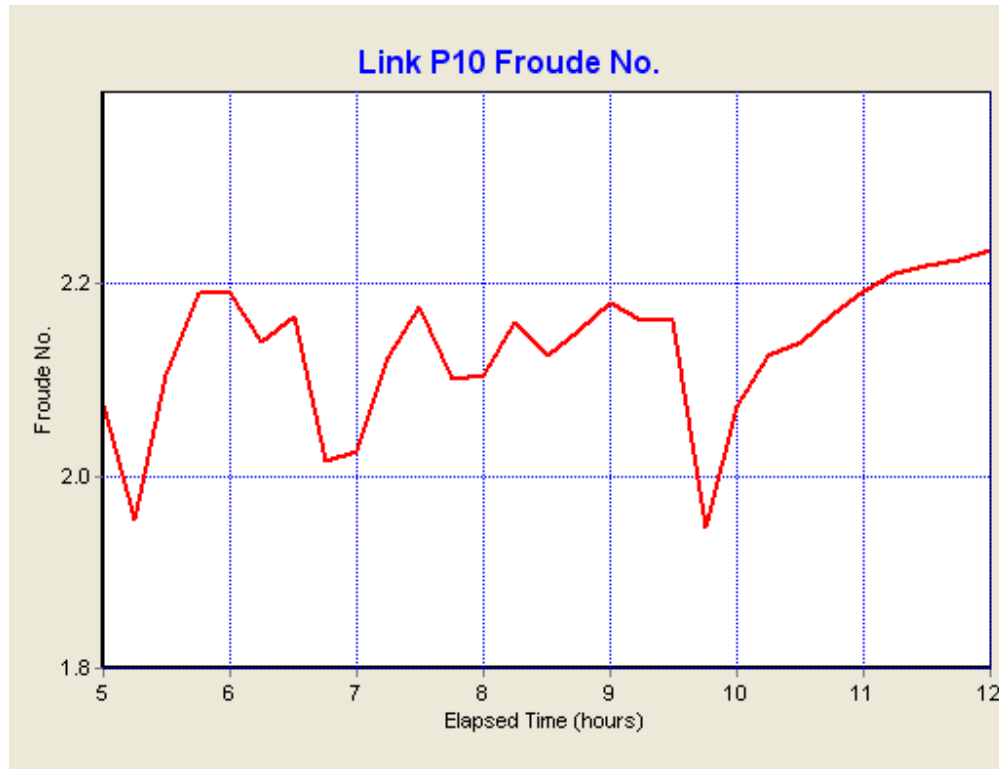


Figure 5.6 The Froude numbers in P10 during M17

The water quality results calculated by SWMM can be reviewed using the status report function of SWMM (Figure 5.7). During the rainfall, flooding had occurred at manhole MH10 for 5 hours. The maximum flooding happened at 9:46, and the total volume of the flooding was 1225 m³. The total TSS mass washed off from catchment was 1776.265 kg. Subcatchment 5 contributed the largest part of TSS mass (384.102 kg), due in part to the fact that it has the largest subcatchment area. The total TSS mass discharged from the outfall was

1633.747 kg, which was about 140 kg less than the mass in the wash-off. The decrease was due to the internal flooding occurred at manhole MH10

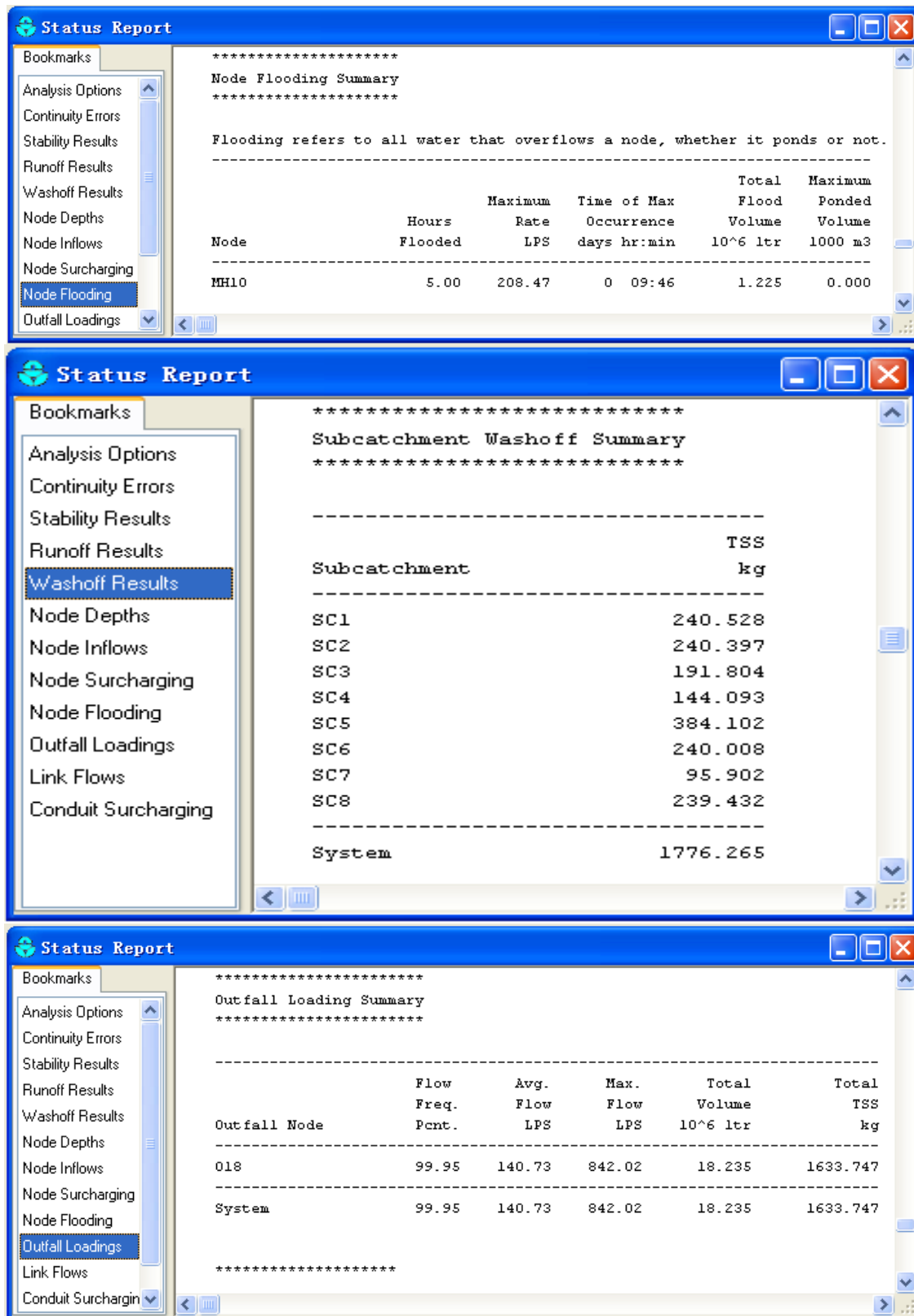


Figure 5.7 SWMM simulation status report

The TSS transport rates were also calculated using EXCEL for a comparison. The particle size was set at 40 μm . Figure 5.8 illustrates the TSS transport rates during the rainfall. The maximum value of transport rate was 0.2609 kg/s at 6:45. Compared to the TSS concentration curve, the higher transport rates also happened during initial period of rainfall event. The effect caused by the first flush of storm runoff was the main reason for this phenomenon. The storm runoff from catchment during the beginning period of rainfall had higher TSS concentration than the runoff in the later rainfall period. The transport rate decreased dramatically after reaching the peak value due to the sharp drop of both TSS concentration and storm runoff after 6:35 hours. From 8:15, the transport rate began to decrease slowly and smoothly. An exception occurred at 9:45 when the transport rate increased to 0.0514 kg/s for 30 minutes. The dramatic increase of discharge in this 30 minutes caused this change of transport curve.

Figure 5.9 shows the TSS transport curve in Le Marais combined sewer system (adopted from Schlutter, 1999). The shape is similar with the calculated curve in figure 5.8. The increase of transport rate also happened at 9:45. The maximum transport rate in Le Marais (0.14 kg/s at 5:45) was much lower and happened earlier than the maximum value of the case study (0.2609 kg/s at 6:45). The error was introduced due to the difference between the Le Marais TSS concentration curves and study sewer system TSS concentration curve. The former curve decreased much more steeply than the later curve. For example, the TSS concentration in case study was 286 mg/l at 7:00. But at the same time,

the TSS concentration in Le Marais system was only 125 mg/l. The steep drop of TSS concentration in Le Marais resulted in the relative lower transport rate between 6:00 and 7:00. The difference between two TSS concentration curves was result from the limitation of wash-off function in SWMM. For the case study, the exponential function was adopted to simulate the TSS wash-off process. The exponential equation was calibrated by two coefficients, C1 and C2. The values of C1 and C2 in case study would be definitely different from the ones in Le Marais due to the different conditions between their catchments, including the surface slope, percent of impervious area, infiltration parameters, etc. The TSS wash-off process affected the TSS concentration in pipes directly and caused the TSS transport errors between two similar combined sewer systems.

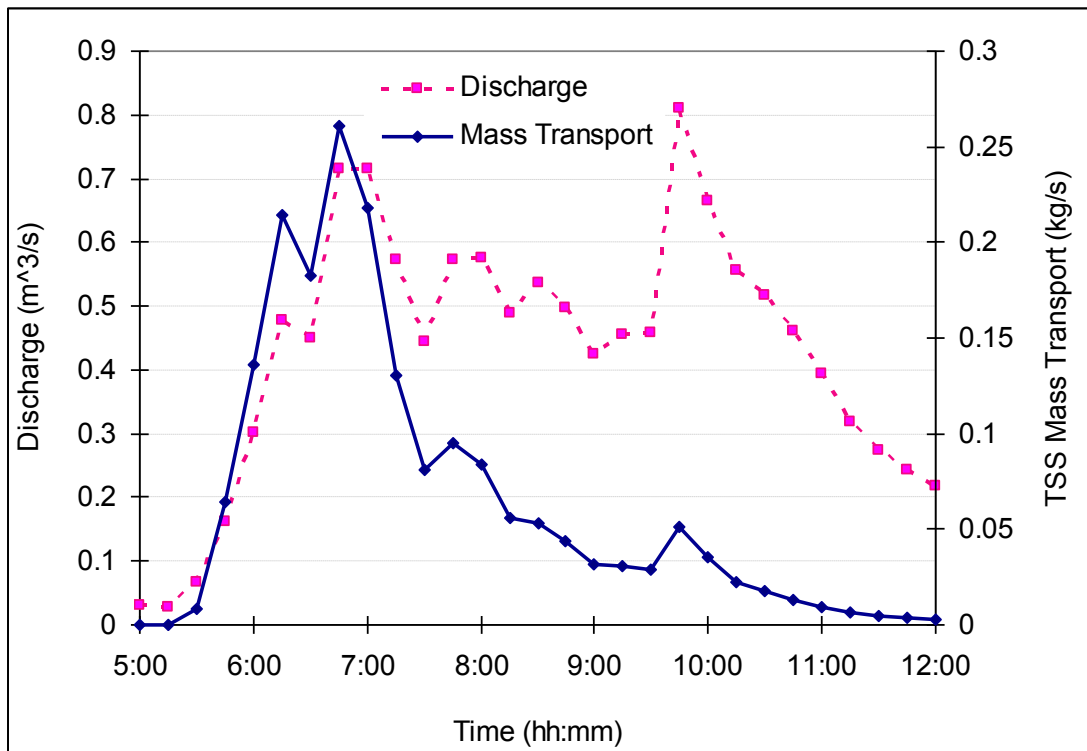


Figure 5.8 TSS transport rates in P10 during M17

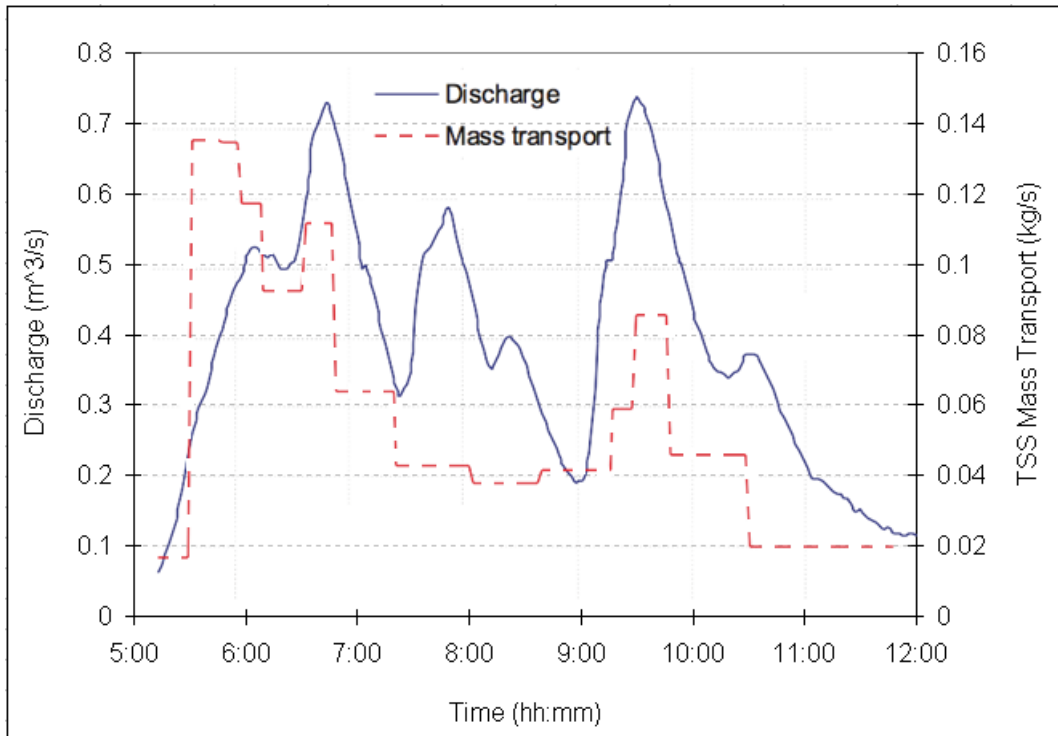


Figure 5.9 TSS transport rates in Le Marais During M17

TSS concentration profile was studied in this work as a part of simplified model. Kaushal and Tomita (2002) also researched the concentration profiles for six particles sizes ranging from 38 μm to 739 μm at three flow velocities, namely 2, 2.75 and 3.5 m/s. Their results demonstrated that solids concentration profiles were a function of particle size, velocity of flow and efflux concentration of slurry. The measured data also shown that there was no significant change with the concentration when y' was ($y' = z/y$) between 0.1 and 0.9. As mentioned in previous chapter, the particle size was set at 40 μm for this case study. The TSS concentration profile in P10 at the transport peak time (6:45) was calculated and plotted in Figure 5.10(a). The water depth in P10 was 0.3803 m at the peak time. The highest concentration was in the bottom area of the pipe. In the vertical

middle area of the pipe ($0.05 \text{ m} < z < 0.35 \text{ m}$), the concentration declined gently and the profile curve changed smoothly.

The effects of particle density on the concentration profile were further evaluated (Figure 5.10(b) and 5.10(c)). The low-density particles (density: 1500 kg/m^3) had a narrow concentration distribution. Most values of concentration were between 330 mg/l and 350 mg/l . But the concentration distribution of high-density particles (density: 3000 kg/m^3) was wider, which was in the range of 290 mg/l to 400 mg/l . This comparison demonstrates that the uniformity of concentration in pipes is inversely proportional to the particle density. If the particle density were equal to the water density, the concentration of TSS would be uniform in the pipe section. This theory can explain the shape of TSS concentration distribution in Figure 5.10(a). The range of concentration was 310 mg/l to 380 mg/l , which was wider than Figure 5.10(b) but narrower than Figure 5.10(c).

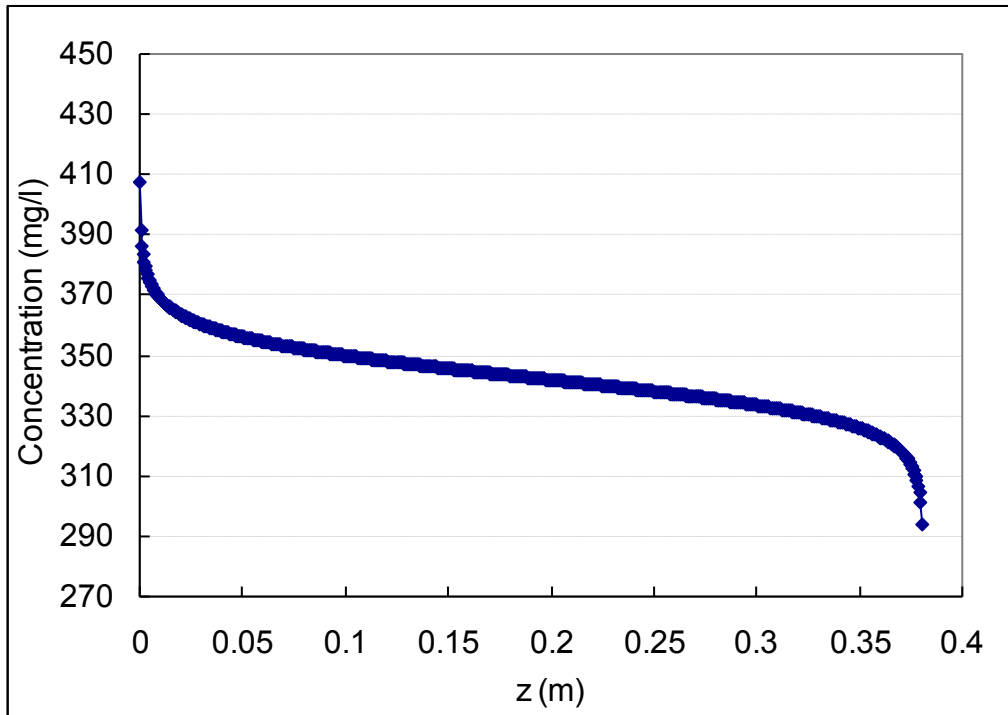


Figure 5.10(a) TSS concentration profile in P10 at 6:45 (density: 2400 kg/m³)

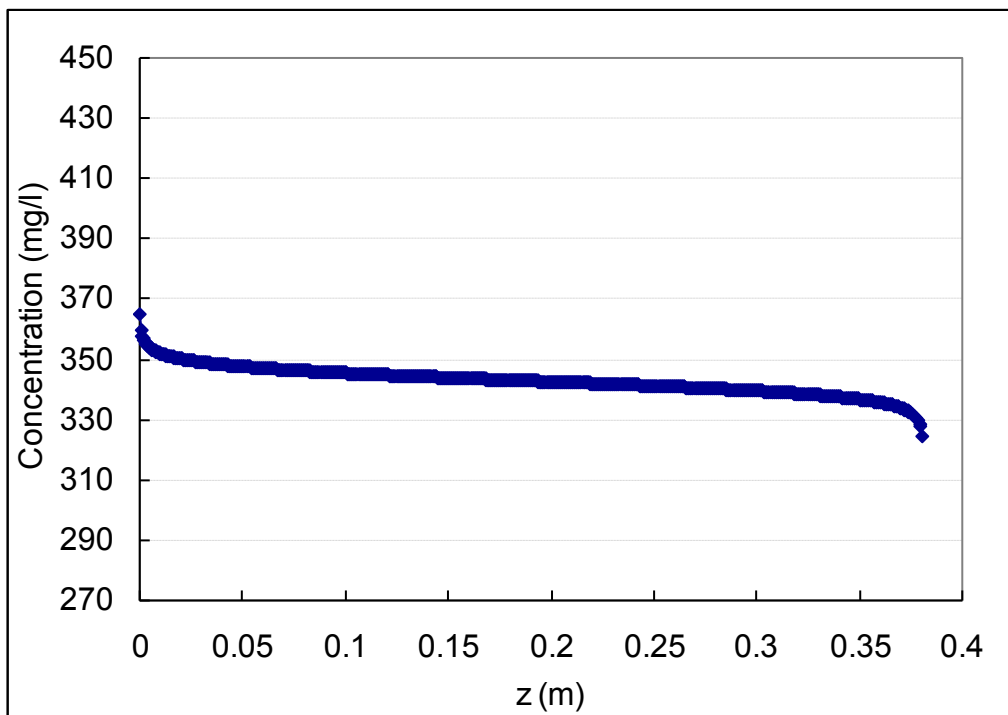


Figure 5.10(b) TSS concentration profile in P10 at 6:45 (density: 1500 kg/m³)

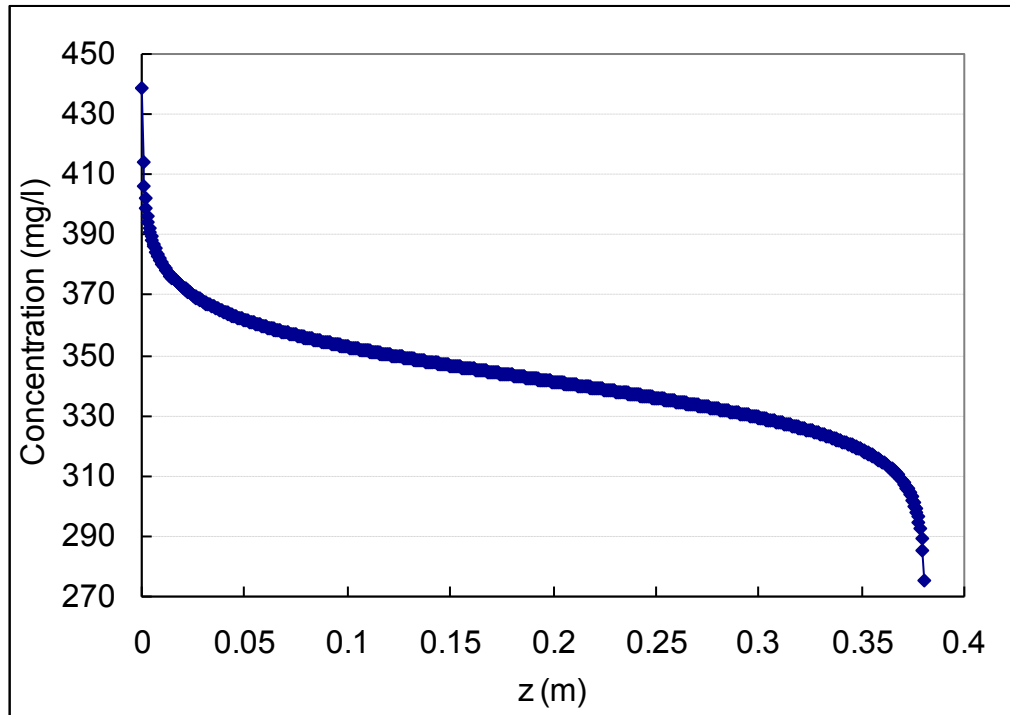


Figure 5.10(c) TSS concentration profile in P10 at 6:45 (density: 3000 kg/m^3)

Figure 5.11 shows the flow velocity profile in P10. Because the maximum flow depth of P10 was less than the diameter of pipe during the entire rainfall process, P10 can be treated as an open channel. Gonzalez et al. (1996) utilized the acoustic Doppler current profiler (ADCP's) to analyze the open channel velocity profile. ADCP is a device uses acoustic pulses to measure water velocities and depth (Morlock, 1996). The ADCP has been commercially available for about 25 years and widely utilized for estuary, river and stream flow measurement, even in weather forecasting. Their analysis based on the velocity distributions in the approximate two-dimensional open channel at Chicago Sanitary and Ship Canal (CSSC) at Romeoville, Illinois. Their results indicated that the logarithmic-law velocity distribution fit well the measured mean velocity profiles of the data set. The flow velocity profile in P10 was also based on the

logarithmic equation (Equation 2.16). So the shape of the curve in Figure 5.11 was reasonable.

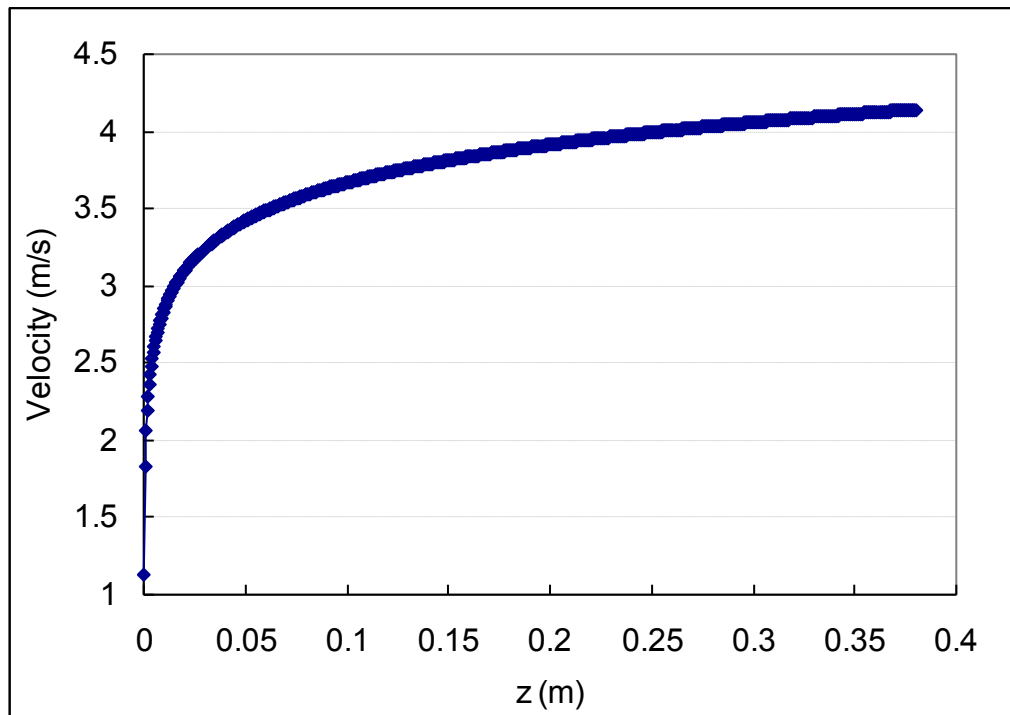


Figure 5.11 Flow velocity profile in P10 at 6:45

Table 5.2 shows the TSS transport rates and some other hydraulic properties of all the pipes in the system at 6:45. Obviously, pipe P5 and P4 had the minimum transport rates (less than 0.02 kg/s). P5 and P4 were located at the beginning part of the collection system. They only received the storm runoff from subcatchment SC7, which had the smallest area in the system evaluated. So the flow and water depth in these two pipes were also lowest in the system. According to the integral equation 2.12, the TSS transport rates in the two pipes should be the lowest. At the same time, the TSS transport rates of P15, P16 and P10 exceeded 0.15 kg/s. P15, P16 and P10 took the largest TSS load because they were located at the end of the combined sewer system. They received the

wastewater not only from the nearby subcatchments but also from the previous pipes they connected. This is especially high for P10, since it received all the wastewater collected in the study area. The TSS transport rate of P10 represents the total TSS transport rate for the entire sewer system evaluated.

Table 5.2 Hydraulic and TSS transport calculation results of all pipes at 6:45

Pipe	Hours	Flow (LPS)	Depth (m)	Velocity (m/s)	TSS transport (kg/s)
P5	6:45	47.9116	0.0738	3.4139	0.016444
P4	6:45	48.2368	0.1091	1.9931	0.016559
P12	6:45	89.4295	0.1563	1.7052	0.032209
P11	6:45	92.2393	0.1389	2.0711	0.032717
P6	6:45	98.6779	0.32	1.227	0.035549
P14	6:45	122.477	0.192	2.4312	0.043286
P1	6:45	134.5413	0.1689	2.3049	0.044062
P7	6:45	145.0622	0.168	2.1326	0.048956
P8	6:45	222.6905	0.2329	2.0835	0.075589
P13	6:45	282.0844	0.3439	1.9592	0.102107
P15	6:45	503.7677	0.3274	3.008	0.178181
P16	6:45	616.8306	0.3721	3.14	0.221274
P10	6:45	714.5751	0.3803	3.543	0.260853

The sensitivity analysis of particle size was also investigated. The median diameter of particles d_{50} changed from 1 μm to 100 μm . The corresponding TSS transport rate in P10 at 6:45 for each d_{50} was calculated using the simplified model. Figure 5.12 illustrates the relationship between the transport rate and median diameter d_{50} . The transport rate curve rose up at first and then dropped down with the increase of d_{50} . There was a maximum value of transport rate in the range of 20 μm to 40 μm . Also the shape of the transport rate curve was parabolic. Therefore, a second order polynomial was used to describe the relationship between d_{50} and TSS transport rate. The coefficient of $n R^2$ was

calculated, since it provides a measure of how well future outcomes are likely to be predicted by the model (Steel and Torrie, 1960). R^2 has a range from 0 to 1. An R^2 of 1 indicates a perfect fit. The R^2 for the model is 0.9836, which indicates that the trendline fits the transport data well. The location of the parabola vertex was calculated by taking the derivative of the polynomial. The result showed the maximum transport rate was 0.2616 kg/s when d_{50} was equal to 35 μm . The transport rates for the particles larger than 100 μm were not calculated in this work. The second order polynomial trendline may be not practical for those rates. But for the suspended solids in the combined sewer pipes, the relationship was described well by this polynomial.

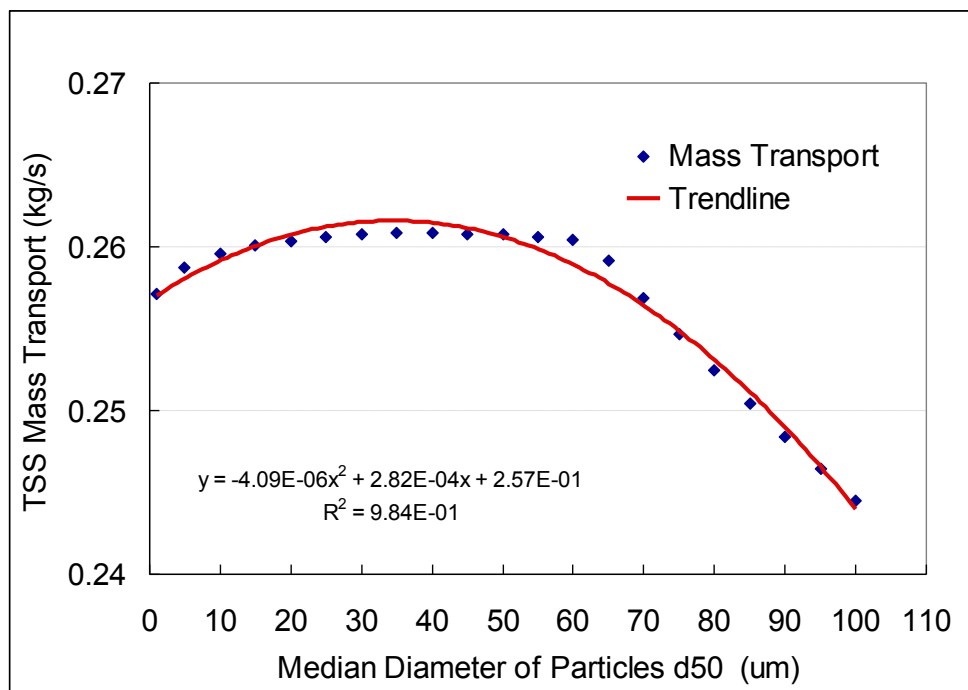


Figure 5.12 Sensitivity analysis of particle size

CHAPTER 6

CONCLUSION

A study was presented that developed a simplified approach for predicting the TSS transport rate in combined sewer pipes. The simplified model was developed using SWMM in combination with EXCEL spreadsheets. Original data sets were attained from the combination of two systems: the rainfall data from a catchment in Le Marais, France and combined sewer system data from SWMM example. The rationality of the combination was validated by the comparison with the measured data from Le Marais. SWMM outputted the TSS concentration pollutograph, while the EXCEL spreadsheets were used to generate the TSS concentration profile and flow velocity profile. The purpose of the two profile graphs was to calculate the TSS transport rate.

The results of SWMM simulation and spreadsheet calculation showed the combined sewer system worked under proper condition during a selected rainfall event (M17), except that flooding occurred at manhole MH5 for 5 hours. The maximum TSS transport rate for the combined sewer system was 0.2609 kg/s at 6:45. As the input of the simplified model, particle density and median particle size d_{50} were used. In addition, the evaluation included sensitivity analysis.. It was determined that the particle density can control the distribution of TSS concentration. It was also determined that the relationship between transport rate and d_{50} can be described by a second order polynomial function.

The selections of equations and parameters for simulating pollutant build-up, wash-off, and transport process were emphasized in this study. All the choices should be based on the local hydraulic and hydrology condition. The difference between the case study transport rate curves and Le Marais transport rate curves reflected this importance.

Future work is needed to collect sufficiently precise field data for calibrating this simplified model. The field data should include rainfall event data, catchment properties, and pollutant concentration in the pipes. The simplified model only studied the suspended solids transported during wet weather period, which were smaller than 100 μm . The transport behaviors of larger particles still needed to be studied.

REFERENCE

- (1) Ashley, R. M., Bertrand-Krajewski, J. L., and Hvived-Jacobsen, T. (2004). *"Solids in Sewers: Characteristics, Effects and Control of Sewer Solids and Associated Pollutants."* IWA Publishing, Alliance House, 12 Caxton Street, London, UK.
- (2) Ashley, R. M., and Crabtree, R. W. (1992). "Sediment origins, deposition and build-up in combined sewer system." *Water Science and Technology*, 25(8), 1-11.
- (3) Bertrand-Krajewski, J.L. (2006). "Modelling of sewer solids production and transport." Cours de DEA *"Hydrology Urban"* part9.
- (4) Bertrand-Krajewski J.L., Chebbo, G., and Saget, A. (1998). "Distribution of pollutant mass vs. volume in stormwater discharges and the first flush phenomenon." *Water Research*, 32(8), 2341-2356.
- (5) Chebbo G., Musquère P., Milisic V., and Bachoc A. (1989). "Caractérisation des solides transférés par temps de pluie dans les réseaux d'assainissement." *Proceedings of the 2nd Wageningen Conference*, Wageningen, NL.
- (6) City and County of Denver. (2006). *"Storm drainage design and technical criteria."*

"<http://www.denvergov.org/Portals/487/documents/Storm%20Drainage%20Design%20and%20Technical%20Criteria%20Manual%20012006.pdf>"

(March 1, 2012).

- (7) Crabtree R. W. (1989). "Sediment in sewers." *Journal of the Institution of Water and Environmental Management*, 3(6), 569-578.
- (8) Crowe, C. T., Elger, D. F., Williams, B. C., and Roberson, J. A. (2009). "*Engineering Fluid Mechanics*." 9th edition. John Wiley & Sons, Incorporated, Hoboken, NJ.
- (9) Dalrymple, R., Hodd, S., and Morin, D. (1975). "Physical and settling characteristics of particulates in storm and sanitary wastewaters." Environmental protection technology series, National Environmental Research Center, Cincinnati, Ohio.
- (10) Dastugue S., Vignoles M., Heughebaert J. C., and Vignoles C. (1990). "Matières en suspension contenues dans les eaux de ruissellement de la ville de Toulouse." TSM, 3, 131-143.
- (11) DHI (1993). "*MOUSE TRAP Technical Reference*." Danish Hydraulic Institute.
- (12) DHI (1997). "*MOUSE Version 4.0 User Manual*." Danish Hydraulic Institute.
- (13) Ellis, J. B. (1986). "Pollutional Aspects of Urban Runoff." NATO ASI series, Vol. G10, 1-38.
- (14) Envirogenics Company. (1970). "In-sewer fixed screening of combined sewer overflows." U.S. Government Printing Office. Washington, DC.
- (15) Gironás, J., Roesner, L. A., and Davis, J. (2009). "Storm water management model applications manual." Office of research and development, U.S. Environmental Protection Agency Cincinnati, OH.
- (16) Gonzalez, J. A., Melching, C. S., and Oberg, K. A. (1996). "Analysis of

- open-channel velocity measurements collected with an acoustic Doppler current profiler." *Rivertech '96-1st International Conference on New/Emerging Concepts for Rivers*, Vol. 1 and 2, 838-845.
- (17) Gupta, K., and Saul, A. J. (1996). "Specific relationships for the first flush load in combined sewer flows." *Water Research*, 30(5), 1244-1252.
- (18) Hogland, W., Berndtsson, R., and Larson M. (1984). "Estimation of quality and pollution load of combined sewer overflow discharge." *Proc. III int. Conf. on Urban Storm Drainage*, Goteborg, Sweden, 841-850.
- (19) Hager, W. H. (1999). "*Wastewater hydraulics*." Springer: Berlin, New York, NY.
- (20) Hager, W. H., and Gissonni, C. (2005). "Supercritical flow in sewer manholes." *Journal of Hydraulic Research*, 43(6), 660-667.
- (21) Kaushal, D. R., and Tomita, Y. (2002). "Solids concentration profiles and pressure drop in pipeline flow of multisized particulate slurries." *International Journal of Multiphase Flow*, 28(10), 1697-1717.
- (22) Krantz, J., and Russell, D. L. (1973). "*Lancaster silo project: particle sizing and density study*." Meridian Eng., Philadelphia, Pa.
- (23) Lessard, P., Beron, P., and Briere, F. (1982). "Estimate of water quality in combined sewers: the Montreal experience." *First Int. Seminar on Urban Drainage System*, 367-375.
- (24) Lin H., and Le Guennec B. (1996). "Sediment transport modelling in combined sewer." *Water Science and Technology*, 33(9), 61-67.
- (25) Litwin Y.J., and Donigian A.S. (1978). "Continuous simulation of nonpoint

- pollution.” *Journal water pollution control federation*, 50, 2348-2361.
- (26) Mark, O. (1995). “Numerical modeling approaches for sediment transport in sewer systems.” thesis, presented to Aalborg University, Aalborg, Denmark, in partial fulfillment of the requirements for the degree of Doctor of Philosophy.
- (27) Morlock, S. E. (1996). “Evaluation of acoustic Doppler current profiler measurements of river discharge.” *Water Resources Investigations Report* 95-4218. United States Geological Survey, Washington, DC.
- (28) Raudkivi, A.J. (1998). “*Loose Boundary Hydraulics*.” Balkema, Rotterdam, Netherlands.
- (29) Rossman, L. (2004). “*Storm water management model user’s manual version 5.0*.” Office of research and development, U.S. Environmental Protection Agency Cincinnati, OH.
- (30) Rouse, H. (1937). "Modern conceptions of the mechanics of fluid turbulence." *Trans., ASCE*, 102, 463-543.
- (31) Schlutter, F. (1999). “Numerical modelling of sediment transport in combined sewer system.” thesis, presented to Aalborg University, in partial fulfillment of the requirements for the degree of Doctor of Philosophy.
- (32) Steel, R. G. D., and Torrie, J. H. (1960). “*Principles and Procedures of Statistics*.” McGraw-Hill, New York, NY.
- (33) U. S. Environmental Protection Agency (2012). “*Storm Water Management Model (SWMM)*.” <<http://www.epa.gov/nrmrl/wswrd/wq/models/swmm>> (March 1, 2012).

- (34) van Rijn L.C. (1984). "Sediment transport, part I : bed load transport." *Journal of Hydraulic Engineering*, 110(10), 1431-1456.
- (35) van Rijn L.C. (1984). "Sediment transport, part II : suspended load transport." *Journal of Hydraulic Engineering*, 110(11), 1613-1641.
- (36) Vanoni, V.A. (1975). "Sedimentation engineering." *ASCE Manual and Report on Engineering Practice* No. 54, New York, NY.
- (37) Verbanck, M. A., Ashley, R. M., and Bachoc, A. (1994). "International Workshop on the origin, occurrence and behavior of sediments in sewer systems: summary of conclusion." *Water Research* 28(1), 187-194.
- (38) Xanthopoulos, C. and Augustin, A. (1992). "Input and Characterization of Sediments in Urban Sewer Systems." *Water Science and Technology*, 25(8): 21-28.
- (39) Zanke, U. (1977). "Berechnung der Sinkgeschwindigkeiten von sedimenten." *Mitt. des Franzius-Instituts fur Wasserbau*, 46(243), Technical University, Hannover, Germany.
- (40) Zug, M., Bellefleur, D., Phan, L., and Scrivener, O. (1998). "Sediment transport model in sewer networks – a new utilization of the velikanov model." *Wat. Sci. Tech.* 37(1), 187-196.

VITA

Graduate School
Southern Illinois University

Weilan Zhang

zhangweilan88@gmail.com

Chongqing University
Bachelor of Science, Water and Wastewater Engineering, June 2010

Thesis Title:
Modeling Total Suspended Solids in Combined Sewer Systems

Major Professor: Dr. Lizette R. Chevalier